ELSEVIER

Imaging Spectroscopy and the Airborne Visible/Infrared Imaging Spectrometer (AVIRIS)

Robert O. Green, Michael L. Eastwood, Charles M. Sarture, Thomas G. Chrien, Mikael Aronsson, Bruce J. Chippendale, Jessica A. Faust, Betina E. Pavri, Christopher J. Chovit, Manuel Solis, Martin R. Olah, and Orlesa Williams

Show Spectra

Imaging spectroscopy is of growing interest as a new approach to Earth remote sensing. The Airborne Visible/Infrared Imaging Spectrometer (AVIRIS) was the first imaging sensor to measure the solar reflected spectrum from 400 nm to 2500 nm at 10 nm intervals. The calibration accuracy and signal-to-noise of AVIRIS remain unique. The AVIRIS system as well as the science research and applications have evolved significantly in recent years. The initial design and upgraded characteristics of the AVIRIS system are described in terms of the sensor, calibration, data system, and flight operation. This update on the characteristics of AVIRIS provides the context for the science research and applications that use AVIRIS data acquired in the past several years. Recent science research and applications are reviewed spanning investigations of atmospheric correction, ecology and vegetation, geology and soils, inland and coastal waters, the atmosphere, snow and ice hydrology, biomass burning, environmental hazards, satellite simulation and calibration, commercial applications, spectral algorithms, human infrastructure, as well as spectral modeling. ©*Elsevier Science Inc., 1998*

INTRODUCTION

Spectroscopy is used in the laboratory in the disciplines of physics, chemistry, and biology to investigate material properties based on the interaction of electromagnetic radiation with matter. Imaging spectroscopy in the solar reflected spectrum was conceived for the same objective, but from the Earth looking and regional perspective (Fig. 1). Molecules and particles of the land, water and atmosphere environments interact with solar energy in the 400–2500 nm spectral region through absorption, reflection, and scattering processes. Imaging spectrometers in the solar reflected spectrum are developed to measure spectra as images in some or all of this portion of this spectrum. These spectral measurements are used to determine constituent composition through the physics and chemistry of spectroscopy for science research and applications over the regional scale of the image.

To pursue the objective of imaging spectroscopy, the Jet Propulsion Laboratory proposed to design and develop the Airborne Visible/Infrared Imaging Spectrometer (AVIRIS) in 1983. AVIRIS first measured spectral images in 1987 and was the first imaging spectrometer to measure the solar reflected spectrum from 400 nm to 2500 nm (Fig. 2). AVIRIS measures upwelling radiance through 224 contiguous spectral channels at 10 nm intervals across the spectrum. These radiance spectra are measured as images of 11 km width and up to 800 km length with 20 m spatial resolution. AVIRIS spectral images are acquired from the Q-bay of a NASA ER-2 aircraft from an altitude of 20,000 m. The spectral, radiometric, and spatial calibration of AVIRIS is determined in laboratory and monitored inflight each year. More than 4 TB of AVIRIS data have been acquired, and the requested data has been calibrated and distributed to investigators since the initial flights.

AVIRIS has measured spectral images for science research and applications in every year since 1987. More than 250 papers and abstracts have been written for the

Jet Propulsion Laboratory, California Institute of Technology, Pasadena, California

Address correspondence to R. O. Green, JPL Mail-Stop 306-438, 4800 Oak Grove Dr., Pasadena, CA 91109-8099. E-mail: rog@gomez.jpl.nasa.gov

Received 24 June 1998; accepted 8 July 1998.

REMOTE SENS. ENVIRON. 65:227–248 (1998)

655 Avenue of the Americas, New York, NY 10010

0034-4257/98/$19.00
PII S0034-4257(98)00064-9

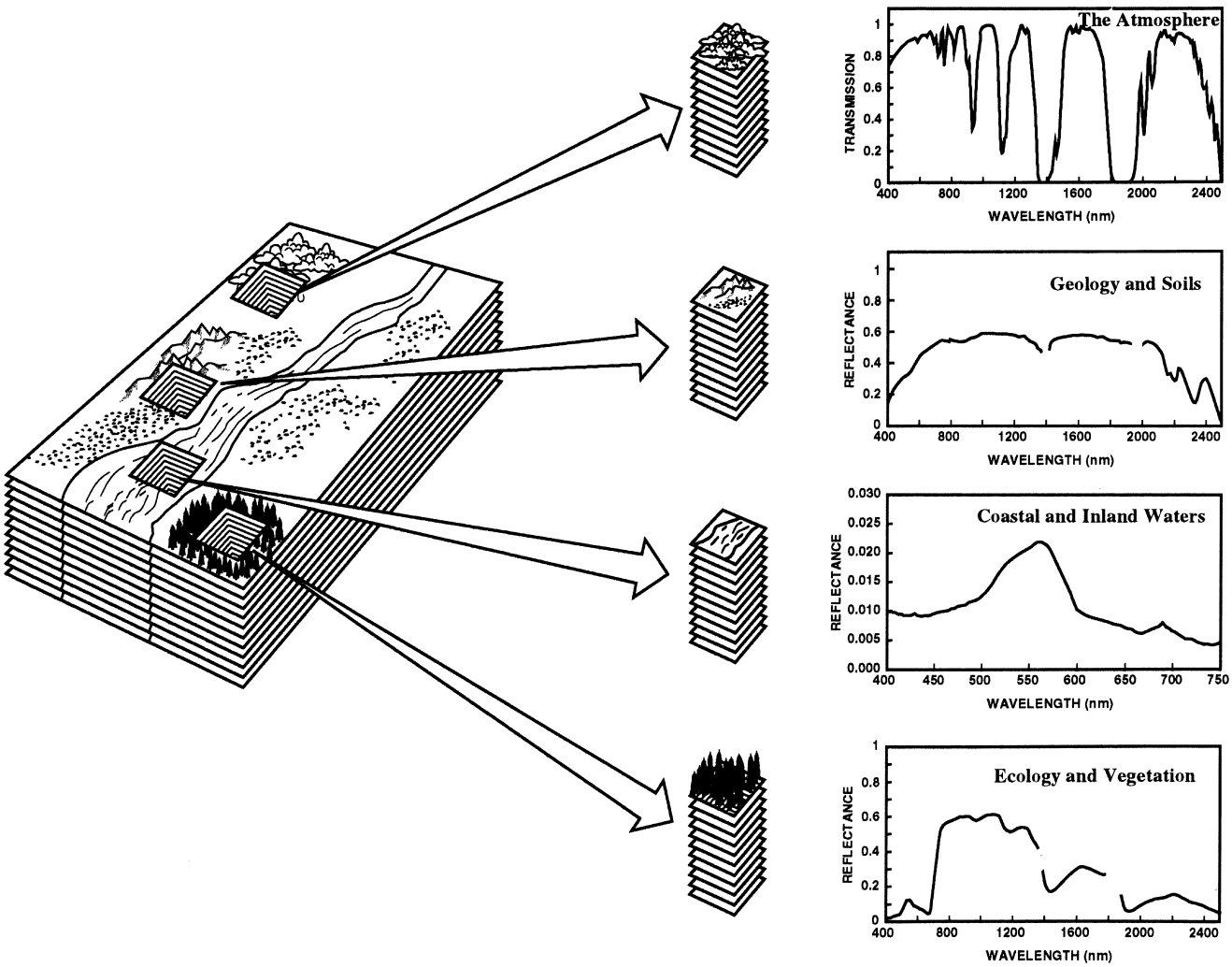

Figure 1. The concept of imaging spectroscopy is shown with a spectrum measured for each spatial element in a image. The spectra are analyzed for science research and applications in a range of disciplines.

AVIRIS workshops (Vane, 1988, Green, 1990a; 1991; 1992; 1993; 1995; 1996a). The workshop documents and additional information are maintained on the AVIRIS website (http://makalu.jpl.nasa.gov/AVIRIS.html). In the past 10 years, there have been a comparable number of AVIRIS papers written for other workshops, symposia, and conferences. A previous special journal issue related to AVIRIS has been published (Vane, 1993). There are additional AVIRIS related articles and papers throughout the remote sensing literature.

The AVIRIS system has been upgraded and improved in a continuous effort to meet the requirements of investigators using AVIRIS spectral images for science research and applications. These improvements have been directed towards the AVIRIS sensor, calibration, data system, and flight operations. In parallel with the sensor, the science research and applications pursued with AVIRIS have diversified and evolved. This article describes the characteristics and recent improvements to the AVIRIS system. The article also reviews a range of science research and applications results and objectives pursued with AVIRIS and provides a context for the accompanying articles in this journal special issue.

SENSOR

AVIRIS is a sophisticated and complex optical sensor system involving a number of major subsystems, components, and characteristics (Table 1). Taken together, these result in the AVIRIS data characteristics (Table 2).

The AVIRIS sensor receives white light in the foreoptics, disperses the light into the spectrum, converts the photons to electrons, amplifies the signal, digitizes the signal and records the data to high density tape. The major subsystems of the sensor are the: scan mirror, foreoptics, spectrometers, detectors, onboard calibrator, and electronic signal chain (Fig. 3). The initial design contained many opportunities for improvements with advances in

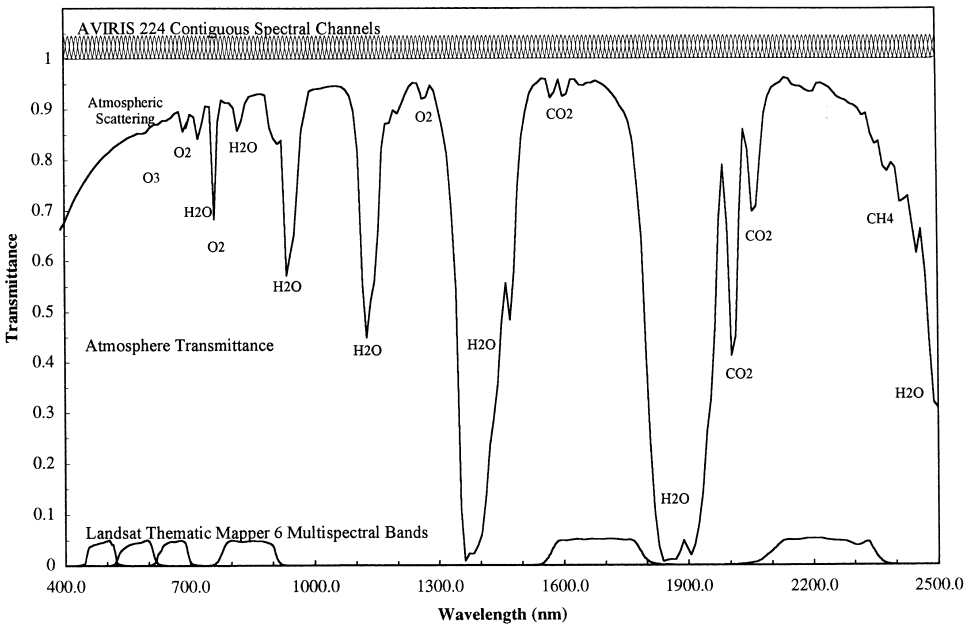

Figure 2. The 224 spectral channels of AVIRIS are shown with a transmittance spectrum of the atmosphere as well as the six solar reflected bands of the Landsat Thematic Mapper.

technology. The initial design, subsequent improvements, and the signal path through AVIRIS are described.

The upwelling radiance arriving at AVIRIS in flight (Fig. 4) enters through at 2.54-cm-thick hatch window in the ER-2 aircraft. This hatch window is composed of low-water fused silica and has an average transmittance of better than 0.95 across the spectrum. An antireflection coating was applied to the hatch window to further improve transmittance. Light arriving from the hatch window passes through the AVIRIS aperture door and is reflected into the foreoptics by an oscillating whiskbroom scan mirror. The aperture door is closed to protect the scan mirror and foreoptics and automatically opened only when spectral images are being measured. The door replaces a protective aperture window that reduced throughput and introduced a small amount of scattered light into the AVIRIS foreoptics. The scan mirror is silver-coated and triangular in cross section with two primary facets giving a 10 cm by 20 cm equivalent area. The oscillating scan drive sweeps the mirror across the active 30° field of view of the Earth at a rate of 12 Hz. Significant engineering effort was required to develop a scan drive to sweep linearly across the 30° field-of-view and then fly back at nearly twice the speed to start the next imaging scan (Miller, 1987). The AVIRIS scan drive approaches 70% efficiency. The great advantage of a whiskbroom scanner is that the light for every spatial element passes through the same path of the optical system. This gives exceptional uniformity for the 614 cross-track spatial samples in each AVIRIS image scan line.

After reflection from the scan mirror the light from the two facets is recombined using a set of fold flats and then focused using a paraboliod and elliptical mirror. A final fold flat is used to direct the focused light to an array of optical fibers. The first three mirrors are coated with high-reflectivity silver, the last two mirrors are aluminum. The 200 mm effective focal length of the foreoptics and the 200 μm diameter entrance aperture of the fibers define the 1 milliradian instantaneous field of view (IFOV) of the AVIRIS sensor. A mechanical shutter is

NOT D.L.

Table 1. AVIRIS Sensor Characteristics

Imager type	Whiskbroom scanner
Scan rate	12 Hz
Dispersion	Four grating spectrometers (A,B,C,D)
Detectors	224 detectors (32, 64, 64, 64) Si and InSb
Digitization	12 bits
Data rate	20.4 mbits/s
Spectrum rate	7300 spectra/s
Data capacity	>10 GB (>8000 km^2)

Table 2. Nominal AVIRIS Data Characteristics

Spectral	
Wavelength range	400–2500 nm
Sampling	10 nm
Spectral response (fwhm)	10 nm
Calibration accuracy	<1 nm
Radiometric	
Radiometric range	0 to maximum lambertian radiance
Sampling	~1 DN noise RMS
Absolute calibration	≥96%
Inter flight stability	≥98%
Signal-to-noise	Exceeding 100:1 requirement
Polarization sensitivity	≤1%
Spatial (at 20 km altitude)	
Field of view	30 degrees (11 km)
Instantaneous FOV	1.0 mrad (20 m)
Calibration accuracy	≤0.1 mrad
Flight line length	800 km total

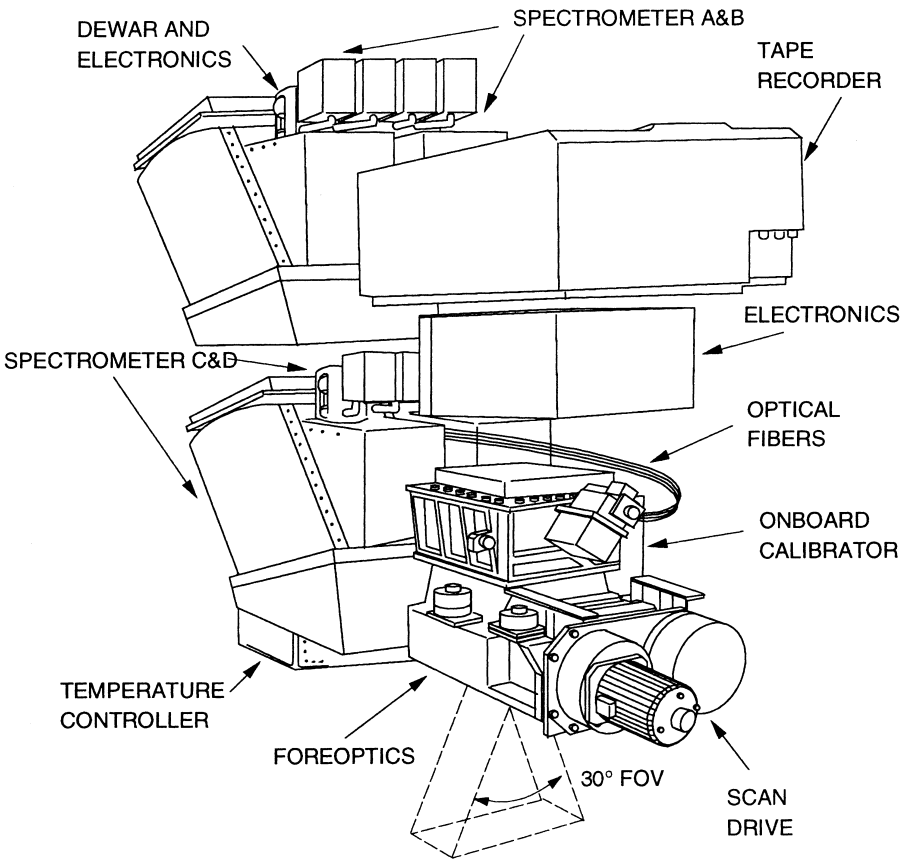

Figure 3. A depiction of the AVIRIS sensor is shown with the major subsystem used to acquire spectral images of the Earth's land, water, and atmosphere environments.

located at the exit of the foreoptics in front of the fiber optics. This shutter closes for the nonimaging portion of each scan line to allow measurement of the dark signal levels. Sixty-four samples of dark signal are averaged for each scan line. Averaging is required to suppress the single sample noise in the dark signal.

Light leaving the foreoptics is focused on four 200-μm diameter optical fibers with 0.45 numerical apertures. These fibers transmit the light to the four spectrometers that are used to cover the spectral range from 400 nm to 2500 nm. Silica glass fibers are used for the range from 400 nm to 1300 nm while Zirconium fluoride glass fibers are used from 1300 nm to 2500 nm. These high numerical aperture exotic glass fibers were specifically

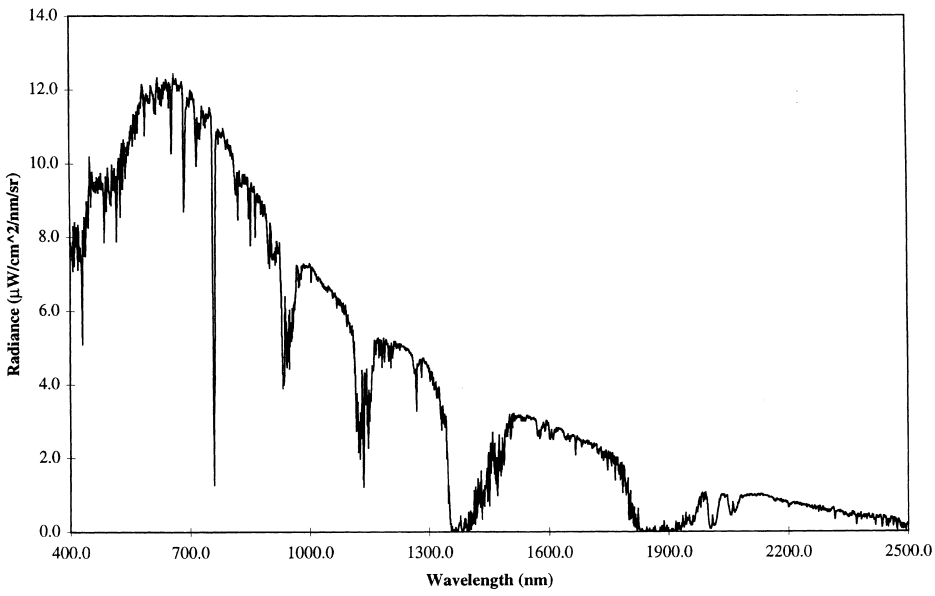

Figure 4. A 1.0 nm spectral resolution modeled upwelling radiance spectrum is given for the Ivanpah Playa, California calibration target in 1997.

developed for AVIRIS and were the first of their kind. However, these fibers are easily damaged by water condensation and water vapor. Several measures were required to isolate the fibers from ambient humidity of the AVIRIS operational environment. These included the placement of sapphire windows on the fiber ends and the development of a dry air unit to provide a high flow source of warm dry air for purging the sensor in humid environments. The use of optical fibers is essential for AVIRIS and enables the independent alignment of the foreoptics and spectrometers as well as the compact packaging required for the ER-2 aircraft.

In the spectrometer subsystem, light from each of the optical fibers enters a different spectrometer covering a portion of the AVIRIS spectral range. The A, B, C, and D spectrometers cover the nominal spectral ranges of 400–700 nm, 700–1300 nm, 1300–1900 nm, and 1900–2500 nm, respectively. These spectrometers are an off-axis Schmidt design. White light from the optical fiber enters each spectrometer with a cone angle of 45°. The light is collimated by a spherical mirror onto a reflection grating where the light is diffracted into the spectrum. The reflection gratings are convex with a correction surface shape unique to each spectrometer. The groove spacing and blaze angle of each reflection grating is optimized for the spectral range of each spectrometer. From the grating the dispersed light reflects from the spherical mirror and is focused on the detector array. The f/1 performance of the AVIRIS spectrometers caused significant optical design and implementation challenges (Macenka and Chrisp, 1987). However, because the solar reflected spectrum is broken into four spectral ranges, each spectrometer could be optimized for the specific spectral range.

The AVIRIS spectrometers are aligned and calibrated in the laboratory at ambient room temperature. At altitude, the Q-bay of the ER-2 may reach temperatures of −10°C. To allow alignment in the laboratory and maintain the performance of the spectrometers in flight, the spectrometers are heated and insulated. In the current improved design, a series of eight heater circuits and temperature probes are used to control the temperature of each spectrometer. A 32 loop thermal control system is used to maintain the temperature of the four AVIRIS spectrometers slightly above laboratory alignment temperatures at all times. Thermal control of the spectrometers is required to maintain the precise optical alignment that is required for spectral and radiometric calibration stability.

Light dispersed into the spectrum by the AVIRIS spectrometers is measured by the detector subsystem. At the exit from each spectrometer, light enters a cryogenic dewar that holds a linear detector array. In front of each detector array is a field flattening lens and a blocking filter. The field flattener helps to achieve sharp focus across the length of the detector array. For each spectrometer a unique blocking filter is used to suppress light of wavelengths not appropriate to the spectrometer. In the D spectrometer a carefully specified linear variable blocking filter is used to limit the wavelengths of light for each element in the detector array. This specialized filter reduces the noise arising from photons emitted by the spectrometer in the 1900–2500 nm spectral range. For the A spectrometer, a 32-element silicon detector array with a blue enhanced response is used. The detector elements are 200 μm 200 μm and operated with the dewar at ambient spectrometer temperature. The B, C, and D spectrometers each have 64-element arrays of indium antimonide detectors. The dimensions of the detectors in the B and C arrays are 200 μm by 200 μm and the quantum efficiency is optimized for the spectral regions. The detector elements in the D spectrometer array are 214 μm by 500 μm in dimension. These larger detectors are used to compensate for astigmatism present in the D spectrometer focal plane. The B, C, and D detector arrays are operated near 77°K. The temperature is controlled by a pressure relief valve attached to the liquid-nitrogen-filled cryogenic dewars. The detector arrays in each spectrometer receive the spectrally dispersed photons and convert them to electrons. The electrons are read off the array elements by buffered direct injection multiplexors that were specifically developed for AVIRIS. New detectors and a new multiplexor design were installed in AVIRIS in 1995. This upgrade resulted in more than a factor of 2 increase in signal-to-noise. Each array is read out every 87 μs to coincide with the motion of the scan mirror through one spatial resolution element. A timing delay in the detector readout is used to align the spectrum from the A, B, C, and D spectrometers to the same spatial sample on the surface. The signals from the detectors are amplified and digitized by the electronics attached to the dewar. The measured AVIRIS signal is digitized at 12 bits and recorded as 224 channels of spectral data (Fig. 5).

A critical subsystem required to achieve the calibration objective of AVIRIS is the onboard calibrator. This subsystem has been upgraded a number of times (Chrien et al., 1995a). Data from the onboard calibrator are measured at the beginning and end of each image flight line. The signal source for the onboard calibrator is a 10-W quartz halogen lamp rated for 5000 h. The intensity of signal from the lamp is stabilized by a silicon detector feedback circuit. The current to the lamp is continuously adjusted to keep the signal measured by the onboard calibrator silicon detector constant. A narrow band filter centered at 543.5 nm wavelength is placed in front of the detector to limit the detector response to a spectral range of temperature insensitivity. To further improve stability, the temperature of the entire onboard calibrator is regulated to 40°C with a dedicated temperature controller. The light from the bulb is passed through a balancing filter to deliver appropriate signal levels across the AVIRIS spectral range. The filtered light is focused on the end of a bundle

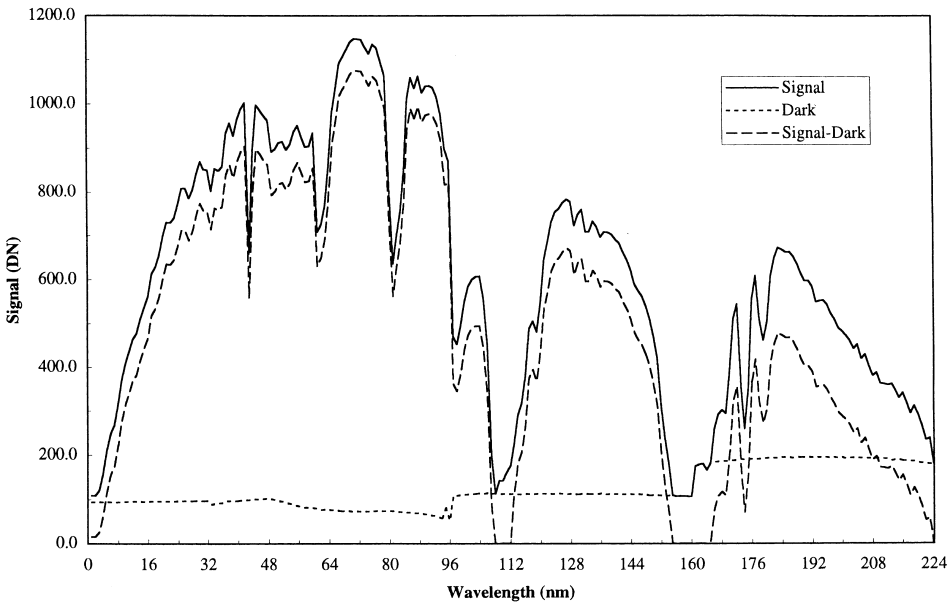

Figure 5. The digitized AVIRIS signal from the calibration target on Ivanpah Playa, California, in 1997 is shown. Also shown are the average dark signal measured in the nonimaging portion of the scan and the difference of the two signals.

of optical fibers. The light is transmitted through the optical fibers to the back of the foreoptics shutter that is also used to measure dark signal. During onboard calibrator data acquisition, the AVIRIS spectrometers measure the light reflected from the back of the shutter. A high signal, two spectral signals, and a dark signal (Fig. 6) measurement are acquired for each onboard calibrator sequence. The signal from the onboard calibrator is used in the calibration of all AVIRIS data and to monitor the spectral and radiometric performance of AVIRIS through the entire flight season.

The AVIRIS electronic signal chain controls the digitized spectra, the engineering data, the navigation data, and the overall operation of AVIRIS. The digitized spectra from each spectrometer are passed into high speed data buffer. In the buffer, data from the A, B, C, and D spectrometers are placed in spectral order. Synchronization and count values are placed in the data stream to identify each spectrum and scan line. Temperatures and voltages as well as other housekeeping signals from the AVIRIS sensor are encoded. Navigation data from a global positioning system sensor and an inertial navigation system are integrated into the data stream. The average dark signal measured with the foreoptics shutter closed during the return scan is added to the data stream. This buffered data stream is passed to the high density tape recorder at a rate of 20.4 megabits per second. The tape recorder holds up to 10.4 GB or 60 min of data. Orchestration of the acquisition AVIRIS spectral images and ancillary data for each flightline is performed

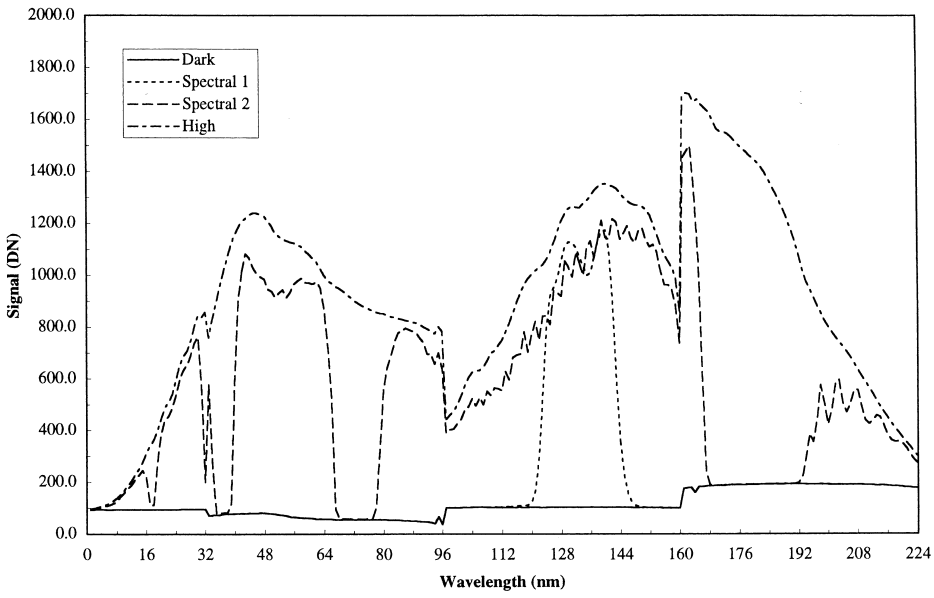

Figure 6. The high, two spectral and dark signals measured from the AVIRIS onboard calibrator are shown for the beginning of the flight line at Ivanpah Playa, California, 1997.

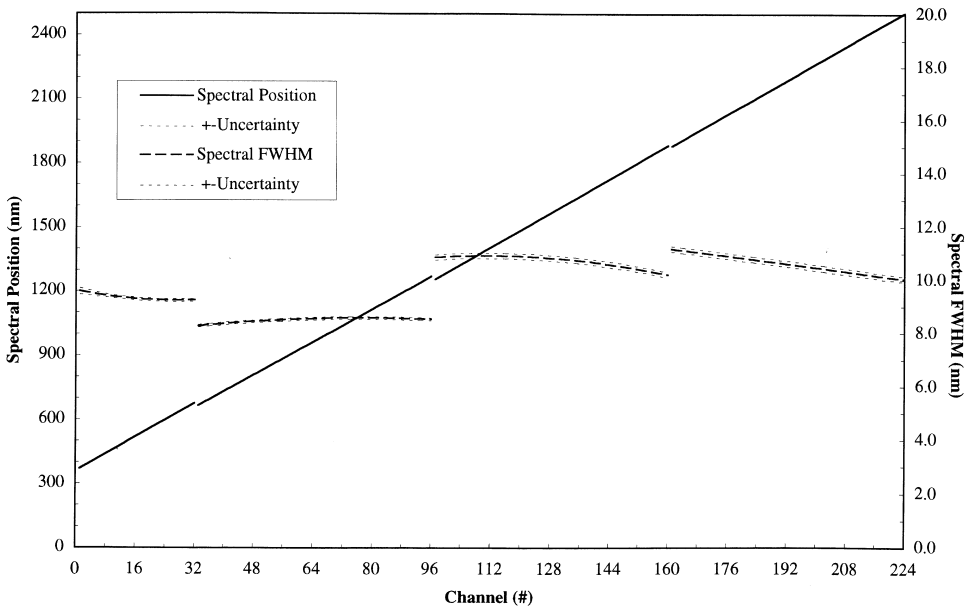

Figure 7. AVIRIS 1997 spectral channel positions and the full width at half maximum response are shown as well as the calculated uncertainties.

by the AVIRIS computer. Because the ER-2 is a single person aircraft, the AVIRIS system is required to be nearly autonomous and collect sufficient monitoring data to allow diagnosis of a wide range of possible problems that could arise in flight.

Typically in each year 8 months are reserved for acquisition of AVIRIS spectral images for science research and applications. In the remaining 4 months, effort is invested towards maintaining and upgrading the performance of AVIRIS. Maintenance objectives are prioritized based on evidence of marginal performance of a subsystem or subsystem component. Upgrade efforts are based on a balance of investigator requirements, advances in technology, and the constraints of the AVIRIS design. Fortunately, the initial AVIRIS design has been well suited to a series of significant upgrades (Chrien et al., 1990; 1993; Chrien, 1992, Sarture et al., 1995).

CALIBRATION

AVIRIS data are required to be spectrally, radiometrically, and spatially calibrated in order to: derive physical parameters from measured radiance; compare data acquired from different regions and from different times; compare and analyze AVIRIS spectra with data acquired by other instruments; and compare and analyze data with results from computer models.

AVIRIS is spectrally, radiometrically, and spatially calibrated in the laboratory before and after each flight season (Chrien et al., 1990; 1995b). At the beginning, middle, and end of the flight season, the calibration of AVIRIS is validated in flight onboard the ER-2. Before and after each AVIRIS flight line, measurements are acquired from the onboard calibrator. This nested set of measurements allows the AVIRIS calibration requirement to be achieved.

In the laboratory, AVIRIS is spectrally calibrated with a computer-controlled three-grating monochromator that covers the solar reflected spectral range. The monochromator is calibrated to the emission lines of low pressure mercury and krypton vapor lamps. Spectral orders of the emission lines are used to calibrate the full monochromator range. These emission lines are the AVIRIS spectral calibration standard. Following the calibration of the monochromator, a quartz halogen lamp is used to illuminate the entrance slit of the monochromator. Light of 1.0 nm spectral width is passed from the monochromator to a collimator that fills the AVIRIS aperture. The monochromator is automatically scanned across each grating at 0.5 nm spectral steps. Simultaneously the measured AVIRIS signal is recorded. The calibrated monochromator input and the AVIRIS measured signals are analyzed with a set of computer programs to determine the spectral positions, response functions, and uncertainties of the 224 AVIRIS spectral channels (Fig. 7). This spectral calibration process was recently automated and may be completed less than 48 h for the 224 spectral channels. Historically, AVIRIS spectral calibration took more than two weeks and required a number of interpolation steps.

The primary AVIRIS radiometric calibration standard is 1000-W quartz halogen lamp with irradiance traced to the National Institutes of Standards and Technology (NIST). The lamp is powered by a regulated power supply of known current and voltage. A new approach has been developed to calibrate AVIRIS with this radiometric standard. A fixture has been constructed that holds the lamp a known distance from a reflectance standard. This fixture also positions the illuminated panel in the AVIRIS field of view and overfills the IFOV. Advantages of this approach are that no transfer spectrometers or radiometers are required and no secondary radiometric

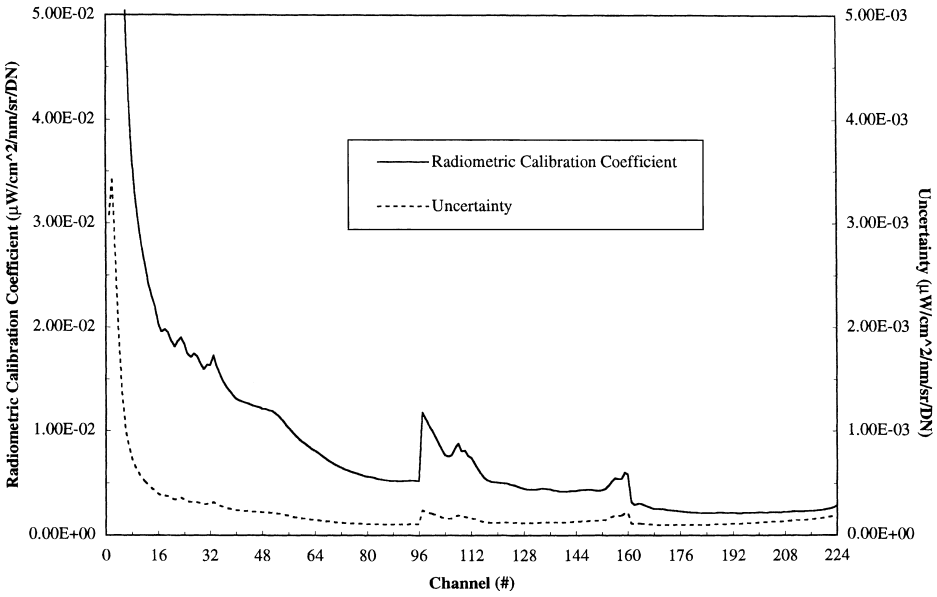

Figure 8. AVIRIS radiometric calibration coefficients and uncertainties are shown for the 1997 flight season.

source is needed. AVIRIS views radiance that arrives from the standard lamp by way of the standard reflectance panel. Use of this method requires careful baffling of scattered light away from the panel as well as knowledge of the bidirectional reflectance properties of the standard panel. Radius and cosine attenuation of the light reflected from the panel must be compensated for as well. The ratio of the known radiance incident at AVIRIS from the panel and the digitized numbers reported by AVIRIS are used to calculate the radiometric calibration coefficients (Fig. 8). In addition to being used in the laboratory, this fixture is used at the ER-2 operation site to monitor and improve absolute radiometric calibration through the flight season. To measure and calibrate the radiometric uniformity across the AVIRIS field of view, a 1-m-diameter integrating sphere with 30-cm aperture is used in the laboratory. An absolute calibration of the integrating sphere is not required. Two additional radiometric calibration standards are being introduced to further improve AVIRIS absolute radiometric calibration. A quantum efficient detector is being used to assess the absolute radiometric calibration accuracy in the visible portion of the spectrum. A metal freezing point blackbody radiation source is being integrated into the radiometric calibration procedures to provide an additional absolute reference in the 1000 to 2500 nm portion of the spectrum.

The radiometric precision or signal-to-noise ratio of AVIRIS is also determined in the laboratory. The average and standard deviation of 3000 dark signal spectra are used to determine the signal chain and background flux noise. The average and standard deviation of an additional 3000 spectra from the illuminated radiometric calibration target are used to calculate the signal dependent photon sampling noise. These two noise components are used to calculate the signal-to-noise for the AVIRIS reference radiance (Fig. 9). The AVIRIS reference radiance was specified in the original AVIRIS proposal to NASA as the radiance from a 0.5 reflectance target illuminated at 23.5° at sea level with the midlatitude standard atmosphere. The current signal-to-noise of AVIRIS is vastly improved over that in 1987 as well as over that in 1994.

The spatial calibration of AVIRIS is measured periodically in the laboratory in a manner analogous to spectral calibration (Chrien and Green, 1993). A quartz halogen lamp is used to illuminate a narrow slit. The illuminated slit is scanned across the focus of a collimator that overfills the AVIRIS aperture. The signal measured by AVIRIS as the slit is scanned is used to determine the spatial response function (Fig. 10). Both the crosstrack and along track spatial response functions are measured. The spatial calibration of AVIRIS is important for investigations examining targets with dimensions near or below AVIRIS spatial resolution.

Field experiments are held at the beginning, middle, and end of the flight season to validate the calibration of AVIRIS in flight from the Q-bay of the ER-2. The initial years of AVIRIS operations demonstrated that a laboratory calibration alone was not sufficient to assure calibration of AVIRIS in flight (Conel et al., 1988a; Green et al., 1988). At this time, the laboratory calibrations did not accurately describe the performance of AVIRIS in the flight operations environment. Inflight calibration validation experiments were developed to assess the calibration of AVIRIS in the Q-bay of the ER-2 (Green et al., 1990; 1996). These experiments acquire *in situ* measurements of the surface and atmosphere at a homogeneous dry lake bed calibration target at the time of AVIRIS spectral image acquisition. Clear sky, low humidity, and low aerosol desert sites are used. The *in situ* measurements are used to constrain the MODTRAN radiative transfer code (Berk

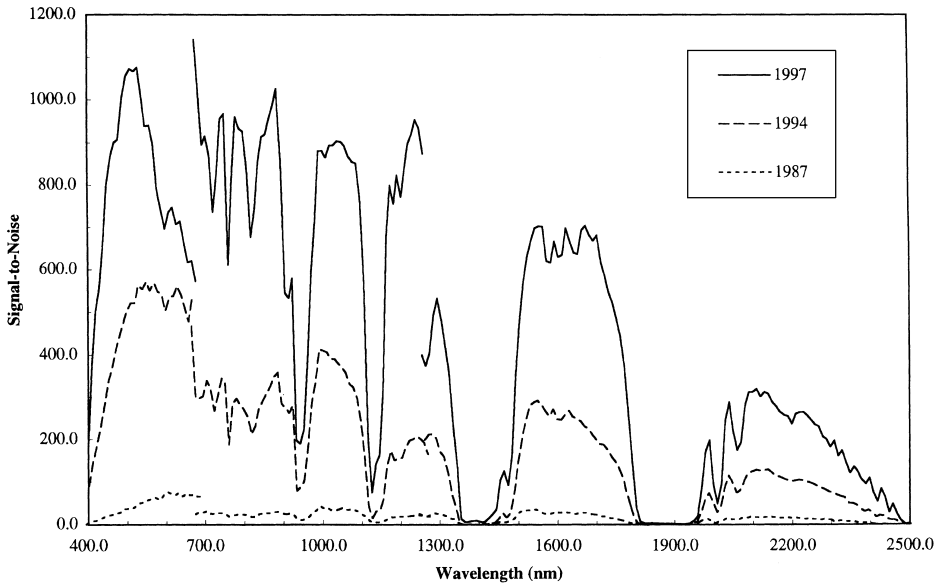

Figure 9. AVIRIS signal-to-noise for 1997, 1994, and 1987 is shown for the reference radiance.

et al., 1989; Anderson et al., 1995) and predict the radiance incident at AVIRIS. The predicted radiance is compared to the AVIRIS-measured radiance traced to the laboratory calibration with the onboard calibrator. The level of agreement between the MODTRAN predicted and the AVIRIS measured radiance is reported to validate AVIRIS calibration in flight (Fig. 11). Since 1995, the average absolute agreement between the predicted and measured radiance has been better than 96%. The residual disagreement must be partitioned among the field measurements, the MODTRAN code, the calibration standards, and the AVIRIS sensor. These experiments are essential to confirm the accuracy of AVIRIS calibration in flight. Science research and applications data sets are only measured in flight.

DATA SYSTEM

The AVIRIS data system contains the computer hardware and software for calibration analysis, performance analysis, trend analysis, archiving, quicklook generation, data calibration, and data distribution. The AVIRIS data system is UNIX-based with software written in standard C and FORTRAN. Prior to 1996, the AVIRIS data system was based on 4 mm archive tapes accessed by hand, a complex relational database, and a monolith data processing program for all years of AVIRIS data. Under this system AVIRIS scenes (140 MB) could be delivered at an average rate of six per day. In 1996 the AVIRIS data system software and hardware had become complicated to the point that the modifications to allow calibration and distribution

good match to pixel size

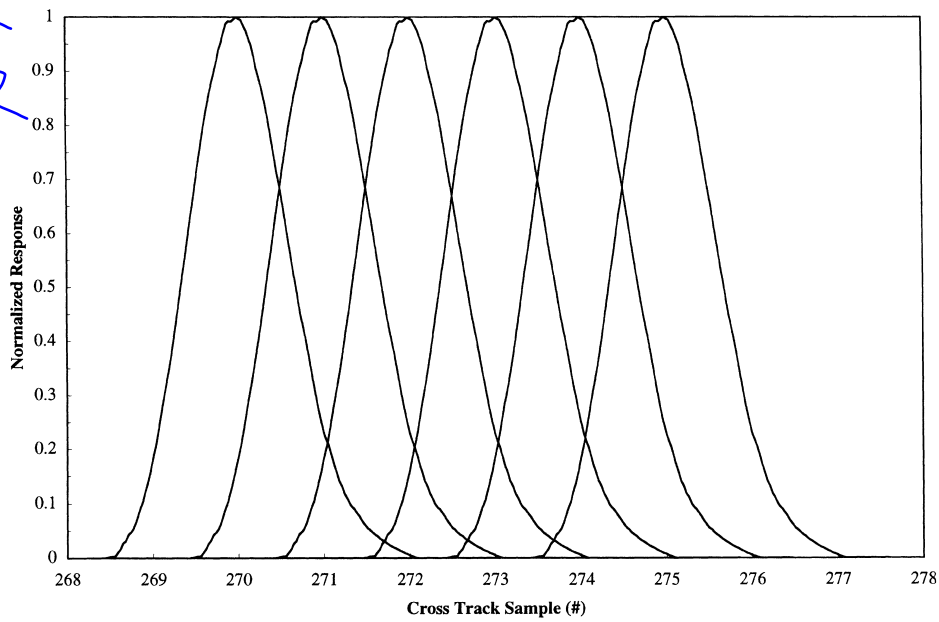

Figure 10. AVIRIS spatial response functions from a portion of the field of view are shown. The sampling is nominally 0.9 mrad and full width at half maximum is 1.0 mrad.

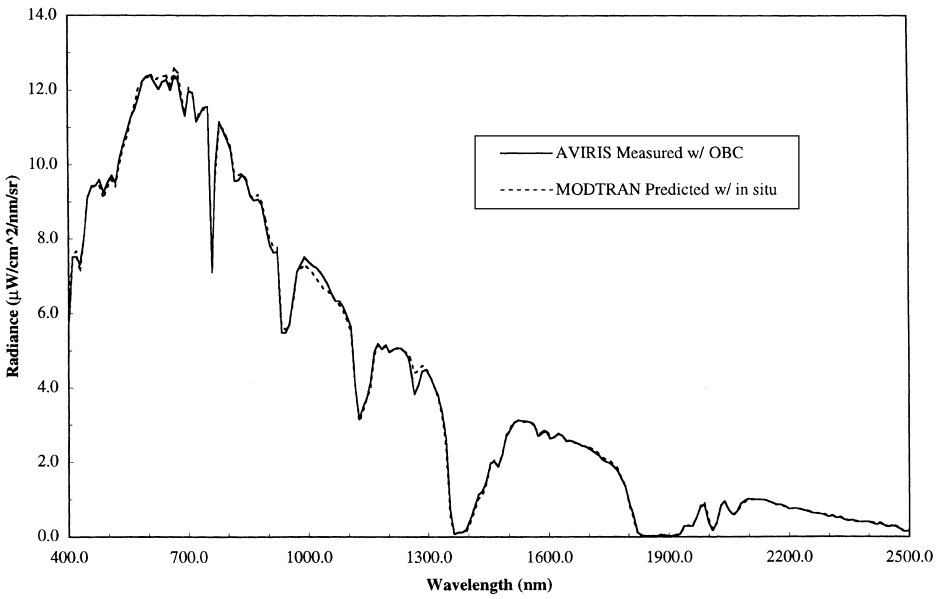

Figure 11. AVIRIS in flight calibration validation result is shown for 1997. The agreement between the MODTRAN predicted radiance and AVIRIS measured radiance for the calibration target is better than 96%.

of 1996 data took almost the entire year. In November 1996 the decision was made to redesign the entire AVIRIS data hardware and software system. The most critical component of the new data system hardware is a 4 TB automated mass storage system. From the perspective of the software and operating system this mass storage device operates as a slow 4-TB disk. The AVIRIS software functionality was redesigned and rewritten as a set of small software modules not dependent on a database. To bypass the database, all file names are based on the date, tape, power cycle, and flight line of the acquired AVIRIS data. This uniquely identifies every data set and is immediately informative. The software modules are divided into four classes, calibration analysis, engineering analysis, routine AVIRIS processing, and experimental AVIRIS algorithms.

AVIRIS data calibration analysis uses a set of software modules that support reduction of laboratory and field calibration data. The radiometric calibration modules allow reduction and analysis of the laboratory radiometric calibration measurements and radiometric standards. These modules sort and distill the more than 3 million AVIRIS spectra acquired during calibration and generate the radiometric calibration coefficients and uncertainties. A set of spectral calibration modules perform the same function for determination of the AVIRIS spectral channel positions, response functions, and uncertainties. Spatial calibration software modules are used to determine the spatial calibration characteristics of AVIRIS. Software modules have also been developed to derive surface and atmosphere parameters from field measurements. These are used for constraint of the radiative transfer code for the validation of AVIRIS calibration in flight. AVIRIS calibration software modules are specialized, interactive, and flexible, but require expert knowledge of the calibration process.

The engineering analysis software for AVIRIS consists of a set of software modules that provide access to the uncalibrated AVIRIS data as well as the engineering and navigation data recorded by AVIRIS. Following acquisition of each AVIRIS high density data tape an engineering performance evaluation module is run. This program reports a selected set of noise, signal, temperature, and scan characteristics of the AVIRIS sensor data. These characteristics are automatically evaluated with a series of pass/fail thresholds. Results are automatically emailed to the lead members of the AVIRIS team. During science flight operations, the performance evaluation software is run within 48 h following each flight. Rigorous performance evaluation has exposed a number of potential or incipient problems before they propagated into the flight data. Trend analysis is a second essential engineering software module. This program extracts information for all the AVIRIS data sets acquired in a year and formats them for statistical analysis and graphical plotting. Parameters such as the onboard calibrator high signal, dark signal, noise, engineering temperatures, and voltages are compiled. The trend analysis module is a powerful tool to assess the quality of AVIRIS data and to explore for subsystems and components that are in need of maintenance. As required, additional specialized engineering software modules are developed to address specific engineering questions.

AVIRIS routine processing modules allow archiving, generation of quicklooks, calibration, and distribution of spectral image data. In the archiving software modules, data from the high density tape are transferred to hard disk as an exact copy of the 12-bit digitized data. A second module expands the 12-bit data to 16-bit integers on disk and generates a header file with specific information about the AVIRIS data set. These 16-bit AVIRIS spectral images

Table 3. Contents of an AVIRIS Distribution Tape

Per flight line (occurs once per tar file/tape)	
*.avhdr	General information about the flight line
*.brz	Browse image of the complete flight line
*.gain	Multiplication factors, radiance to 16-bit integer
*.geo	Geometric calibration data
*.log	Log information of the distribution processing
*.occ	Onboard calibration correction coefficients
*.post	Post flight line onboard calibrator data
*.pre	Preflight line onboard calibrator data
*.rcc	Radiometric calibration coefficients
*.readme	Explanation
*.spc	Spectral calibration file
Per scene (occurs once or several times per tar file/tape)	
*.drk1	First part of summed dark signal
*.drk2	Second part of summed dark signal
*.eng	Engineering data
*.nav	Navigation data
*.img	Calibrated AVIRIS radiance (image) data

are copied to the automated mass storage device. Following archiving of AVIRIS data, a quicklook image is generated. The quicklook image is a single AVIRIS spectral channel stretched at 512 scanline intervals. The quicklook is placed on the AVIRIS web site along with an index that contains site names and location information. The calibration module retrieves the 16-bit data from the automated mass storage device and applies the calibration algorithms to the data. Calibrated AVIRIS data are written to hard disk with all the associated calibration, engineering, and navigation information as separate files. The distribution program is the final module. This program reads the calibrated AVIRIS data and divides the flight line into a series of 512 scanline image scenes. The scenes and ancillary files are written to a standard UNIX TAR file (Table 3). The TAR file is copied to tape and sent to the requesting investigator. The new AVIRIS calibration and distribution software and hardware have sufficient performance to allow automatic calibration and distribution of all measured AVIRIS data to the investigators. This procedure was adopted in 1997, and all measured AVIRIS data were delivered.

With the installation of new hardware and development of new AVIRIS software modules, a number of experimental algorithms are enabled. For example, a four-module automated reflectance inversion algorithm has been implemented. The code accepts information from the AVIRIS navigation file and performs a series of radiative transfer calculations to model a range of possible atmospheric conditions with variations in water vapor and aerosols. The navigation data are used to access the surface elevation data from a global topographic data set. As second module convolves the radiative transfer calculated spectra to the AVIRIS spectral characteristics and reduces the calculated spectra to an analytical function based on the water vapor and aerosol parameters. The third module performs a nonlinear least-squares spectral fit between the AVIRIS-measured spectra and the modeled spectra to derive the water vapor for each spatial element in the AVIRIS image. The final module performs a full inversion of the measured radiance to surface reflectance. This software is currently run for selected reflectance inversion validation data sets. Another experimental software module accesses the automated mass storage system to reprocess an entire flight season of AVIRIS data to test for cirrus cloud contamination. The algorithm generates a quicklook image from the 1380 nm AVIRIS channel where cirrus clouds are strongly expressed. Another experimental software module was developed to examine every AVIRIS spectrum measured during the 1995 deployment to Brazil. The algorithm tests for the presence of actively burning fire and reports the location and spectrum. Additional broadly posed questions are possible now that an entire flight season of AVIRIS data is accessible through the automated mass storage system.

The recent vast improvement in the AVIRIS data system arises from the modular software design and automated mass storage technology. Since data distribution began on the new system, more than 4500 AVIRIS scenes or 630 GB have been distributed to investigators. A peak throughput of 180 calibrated AVIRIS scenes was achieved in a single day. As part of the migration to the new data system, all AVIRIS data measured from 1992 to present are being rearchived and made available in the new format. The automated mass storage basis of the system will enable easy migration to new mass storage technology in the future. Also, the entire AVIRIS data set may be replicated for long-term data storage at an alternate location. The new AVIRIS data system is being used as the basis for the ground data systems of several proposed spaceborne imaging spectrometers.

FLIGHT OPERATIONS

The objective of AVIRIS is to measure imaging spectroscopy data for science research and applications. This objective is only achieved when AVIRIS is operating from the Q-bay of the NASA ER-2 aircraft (Table 4). For typically eight months of each year, AVIRIS is deployed and collecting data sets with the ER-2. Following laboratory calibration, AVIRIS is shipped to the ER-2 operation site

Table 4. Nominal ER-2 Aircraft Characteristics for AVIRIS

Aircraft	NASA ER-2
Altitude	20 km
Temperature	−10°C to 50°C
Velocity	730 km/h
Pressure	1013 millibar to 280 millibar
Range	2100 km
Flight duration	6.5 h
Launch sites	Domestic and foreign

with a complete set of ground support equipment. The first flight following a period of engineering maintenance is dedicated an inflight calibration validation experiment. Once the first flight is complete and AVIRIS performance validated, the flight season commences. In the weeks and months preceding shipping, a database of approved investigators is reviewed by the AVIRIS experiment coordinator and the ER-2 pilots. The list of approved AVIRIS data acquisitions is maintained on the AVIRIS Web site. Investigators are contacted and requested to review the planned flight lines. On the day prior to each planned flight day, the possible data acquisitions are determined and reviewed at a 1 p.m. meeting. Nominal targets for the following day are selected based on the investigator requests, predicted weather, aircraft status, and AVIRIS status. Following the 1 p.m. meeting, investigators are informed of the plans for acquisition of their data.

On the morning of the flight, 4 h prior to takeoff the preflight preparation and checkout of AVIRIS begins. The AVIRIS sensor is uploaded into the ER-2 aircraft, if necessary. Ground power is applied to the sensor through the aircraft, and the cryogenic detector dewars are filled with liquid nitrogen. A tape is inserted in the high density tape recorder, and series of commands are issued to AVIRIS from the ground support computer. These commands format the tape and collect signals from the onboard calibrator and other subsystems of AVIRIS. Voltages, currents, temperatures, and signal levels are checked to confirm that AVIRIS is operating within specification. A test data set is recorded to confirm the end-to-end operation of AVIRIS. In this period the regional weather is reviewed, and the final decision is made for data acquisitions. Investigators are contacted by the AVIRIS experiment coordinator. Data from one to four investigators may be acquired on a single flight. In the hour prior to takeoff the pilot enters the ER-2 and the engine is started to provide aircraft power. On the runway immediately prior to takeoff, AVIRIS is turned on, and the pilot acquires a small AVIRIS data set to confirm sensor operation.

Once airborne, the pilot proceeds to the planned acquisition sites. Typically, AVIRIS data sets are acquired from one latitude and longitude point to another as specified by the investigator. The pilot notes the location and time of each flight line as well as the cloud and haze conditions. An AVIRIS flight may last 6.5 h and range more than 2000 km from the operations base. As the pilot returns to the operations base a final data set is acquired at altitude to record the performance of AVIRIS at the end of the mission. Once on the ground, the AVIRIS warm/dry air unit is connected to the ER-2 to eliminate the risk of water condensation damage. After warm up, the ground computer is connected to AVIRIS, the post-flight performance evaluated, and the flight tape ejected. The AVIRIS experiment coordinator reviews the flight with the pilot and completes a flight log that relates the record cycles on the tape to the data sets acquired. The flight log and high density tape are express-shipped to the AVIRIS data system. Within 48 h of acquisition, the flight data are evaluated, and the results reported to the experiment coordinator and the pilot.

These flight operation procedures are repeated through the 8-month data acquisition period. During the flight season AVIRIS is usually deployed to two or three bases of operation with the ER-2. These bases are typically east coast and midcontinent. Each deployment entails significant shipping and coordination logistics. AVIRIS has been deployed outside the conterminous United States in Europe, Alaska, and Brazil.

RESEARCH AND APPLICATIONS

AVIRIS has measured spectral images for research and applications since the late 1980s. Both the calibration and signal-to-noise ratio of AVIRIS has improved each year since the initial flights. In parallel to the upgrades to the AVIRIS system, there has been improvements in our understanding of the spectral characteristics of materials in the land, water, and the atmosphere. The improved sensor system characteristics and understanding of the spectrum have enabled a wide range of science research and applications based on spectral images measured by AVIRIS. A review of some of these investigations with AVIRIS spectral images is given. The number and diversity of investigations continues to grow each year.

Atmospheric Correction

AVIRIS measures the total upwelling spectral radiance at 20 km altitude above the surface. The majority of investigations using AVIRIS data for research and applications are pursuing questions whose answers are expressed in the reflectance of the surface. Strategies, algorithms, and approaches for atmospheric correction and derivation of surface reflectance are essential for these investigations. The empirical line atmospheric correction was one of the first methods applied to AVIRIS data (Elvidge, 1988). For this method, the reflectance of two or more targets in the AVIRIS data set are independently measured. A linear relationship is determined between the AVIRIS measurement and the known reflectance of the targets. This relationship is used to transform the entire AVIRIS data set to reflectance. Strengths of this approach are that absolute radiometric calibration of the sensor data is not required. Drawbacks of this approach are the need for concurrent *in situ* spectral reflectance measurements and the failure to account for lateral and temporal variations in the atmosphere.

To move beyond the need for *in situ* measurements, radiative transfer atmospheric correction algorithms have been developed. These algorithms derive the spatial distribution of water vapor, aerosols, and other atmospheric

constituents from the AVIRIS spectra. With these atmospheric constraints an inversion from radiance to reflectance for each AVIRIS spectrum is performed (Green, 1990b; Gao et al., 1991a; 1993; Green et al., 1993; Zagolski and Gastellu-Etchegorry, 1995; Leprieur et al., 1995; Gaddis et al., 1996; Staenz et al., 1996). Several of these methods have been compared in research studies (Farrand et al., 1994; Clark et al., 1995). With these radiative transfer based methods, there are differences between the radiative transfer calculations and the calibrated AVIRIS spectra. These differences cause residual spectral artifacts in the derived reflectance. A number of strategies have been developed to suppress these artifacts. One method requires independent knowledge of the reflectance of at least one target in the AVIRIS data set (Clark et al., 1995). Work is continuing to bring the radiative transfer calculations and AVIRIS measurements into closer agreement. The advantage of these radiative transfer reflectance inversion methods is that *in situ* surface measurements are not required.

Ecology and Vegetation

Ecology and the study of terrestrial vegetation are important objectives for research with AVIRIS spectral images. Leaf water, chlorophyll, ancillary pigments, cellulose, lignin, and other constituents in conjunction with the leaf and canopy structure combine to produce the reflectance of vegetation as measured by AVIRIS. Leaf water is an important vegetation constituent with absorption bands at five locations in the solar reflected spectrum. AVIRIS has been used to measure the expressed leaf water in vegetation (Green et al., 1991; Gao et al., 1991b; Roberts et al., 1993; Gao and Goetz, 1995; Ustin et al., 1998). The nonphotosynthetic fraction of vegetation was not previously measured with remote sensing methods. Analyses with AVIRIS using the full spectrum has enabled the separation and measurement of the nonphotosynthetic components of vegetation (Roberts et al., 1990; 1993; Ustin et al., 1992; Gao and Goetz, 1994). Remote sensing determined canopy chemistry may allow measurement and monitoring of changes in plant function with changes in the atmosphere and the climate. A number of research investigations have focused on the use of AVIRIS spectral images for canopy chemistry (Martin et al., 1993; Gastellu-Etchegorry et al., 1995; Kupiec and Curran, 1995; Martin and Aber, 1997; Curran et al., 1997). Canopy chemistry investigations have benefited from the high signal-to-noise of recent AVIRIS data. AVIRIS spectral measurements have been used to determine ecological patterns of use and productivity in vegetated regions (Gamon et al., 1992; Ustin et al., 1996; Wessman et al., 1997; Roberts et al., 1997). Detection of trace quantities of vegetation has been pursued with AVIRIS (Elvidge, 1990; Chen et al., 1992; Elvidge et al., 1993), as well as assessment of vegetation fraction (Sabol et al., 1993; Garciaharo et al., 1996) and measures of canopy closure (Staenz et al., 1993). The identification of vegetation type and in some cases identification of species has been demonstrated with calibrated and high signal-to-noise AVIRIS spectral images (Martin et al., 1998; Roberts et al., 1998). Research is continuing to understand the relationship between vegetation spectral reflectance and leaf chemistry and structure as well as plant and canopy architecture. Understanding of these relationships is essential for expansion and quantification of the ecological research and applications based on calibrated AVIRIS spectral images.

Geology and Soils

The application of AVIRIS spectra to geology and soil investigations is based on the large number of minerals with unique spectral absorption features in the solar reflected spectrum. AVIRIS has been used to determine the point, local, and regional distribution of minerals for a range of geology and soil science investigations. A class of minerals with strong molecular absorption features is associated with hydrothermal alteration. These minerals have been mapped in a range of investigations with AVIRIS (Carrere and Abrams, 1988; Hook and Rast, 1990; Swayze et al., 1992; Sommer et al., 1993; Boardman and Huntington, 1996; Farrand, 1997; Beratan et al., 1997). AVIRIS spectra have been used to map ammonium minerals (Baugh et al., 1995; 1998). Alkaline and carbonatite rock types have been mapped with AVIRIS (Rowen et al., 1995; Bowers and Rowan, 1996). Carbonate, clay, iron oxide minerals found in sedimentary rocks enable spectroscopic mapping of the units and subunits with AVIRIS (Boardman and Goetz, 1991; Clark et al., 1992; Lang and Cabral Cano, 1996). Evaporite minerals possess spectral absorption features in the AVIRIS spectral range that have been used to map these sedimentary units (Crowley, 1993). An interesting application of imaging spectroscopy to active igneous geology is the measurement of the temperature of exposed lava and volcanic hot spots (Oppenheimer et al., 1993). The radiance emitted by the hot lava is uniquely expressed in the AVIRIS spectrum. As with rocks, the mineral absorption and scattering characteristics of soils are expressed in the AVIRIS spectral ranges. Absorption features in soils tend to be subtle due to particle size, scattering and coating effects. AVIRIS spectra have been used to map the distribution and relationship between soil sequences and other surface materials (Fox et al., 1990; Fischer, 1991; Mustard, 1993; Palaciosorueta and Ustin, 1996). The improved signal-to-noise of AVIRIS supports mapping more subtly expressed minerals as well as mapping several minerals mixed within a single AVIRIS spectrum of the surface. AVIRIS spectral images are suited to any geology or soil research or application question that is posed in terms of the distribution of minerals exposed at the surface.

Coastal and Inland Waters

The number of absorbing and scattering components found in the coastal ocean, lakes, and rivers supports the use of spectroscopy to isolate and measure the constituents of these environments. These constituents include: chlorophyll, a wide range of planktonic species, dissolved organics, suspended sediments with local and distant sources, bottom composition, submerged aquatic vegetation, etc. AVIRIS spectra and *in situ* measurements have been used to investigate the distribution of constituents in lake systems (Melack and Gastil, 1992; Jaquet et al., 1994; Novo et al., 1995). In the coastal environment AVIRIS spectra have been used to investigate coastal ocean reflectance (Pilorz and Davis, 1990), algal blooms (Richardson et al., 1994), sediment plumes (Carder et al., 1993), and bathymetry (Sandidge and Holyer, 1998). The increased signal-to-noise and absolute calibration of AVIRIS in the 400–1000 nm portion of the spectrum is supporting new investigations in the coastal and inland water environments.

The Atmosphere

The molecular and particle constituents of the atmosphere are strongly expressed in the solar reflected spectra measured by AVIRIS. These constituents include water vapor, carbon dioxide, oxygen, clouds, aerosols, ozone, and other atmospheric gases. Water vapor is of interest as a critical component of the atmosphere and as the primary absorber across the AVIRIS spectral range. A number of algorithms and approaches have been developed for derivation and analysis of water vapor (Conel et al., 1988b; Green et al., 1991; Gao et al., 1991b; Bruegge et al., 1992; Schläpfer et al., 1998). In general, these algorithms assess the strength of the 940 nm water vapor absorption and relate the strength to the total column water abundance of the atmosphere. AVIRIS-derived water vapor is an essential input to model based reflectance inversion and is of interest for understanding the spatial and temporal distribution of this atmospheric component (Green and Conel, 1995).

Cirrus clouds play an important role in the global energy balance and are often an undetected confounding factor in remote sensing data. AVIRIS spectral images in the strong water vapor absorptions at 1380 nm and 1850 nm provide a new approach to detect the presence and distribution of cirrus clouds (Gao and Goetz, 1992; Gao and Kaufman, 1995; Hutchison and Chloe, 1996). Algorithms have been developed to assess and compensate for the effects of cirrus clouds in AVIRIS spectral images (van den Bosch et al., 1993). Non-cirrus-cloud fraction and cloud shadow analyses have been pursued with AVIRIS (Gao and Goetz, 1990; Kou et al., 1990; Berendes et al., 1991; Feind and Welch, 1995). Recently, the MODTRAN radiative transfer code has been improved to more accurately model the expression of clouds in the solar reflected spectrum (Berk et al., 1998). Measurement of aerosols is of interest for understanding their impacts on the local and global atmosphere and climate. Knowledge or estimation of aerosols is required for atmospheric correction of imaging spectroscopy and other remote sensing data. Aerosols are expressed in the AVIRIS spectral range and have been a topic of investigation (Isakov et al., 1996; Kaufman et al., 1997). Whether focused on the surface or the atmosphere, all investigations with AVIRIS must account for the atmosphere. Research in this discipline continues to expand and be strongly relevant.

mention MIe

Snow and Ice Hydrology

Properties of snow and ice expressed in the AVIRIS spectral range are: fractional cover, grainsize, surface liquid water content, impurities, and shallow depth. Snow grainsize is required to model the albedo of snow. Snow albedo plays a significant role in the regional and global energy balance. Derivation of snow grainsize has been pursued with AVIRIS spectra (Nolin and Dozier, 1993). Liquid water in melting snow has been shown to modify the solar reflected spectrum of snow (Green and Dozier, 1995). Radiative transfer model based methods have been pursued to derive the snow grainsize and liquid water content simultaneously from spectra measured by AVIRIS (Green and Dozier, 1996). Advanced methods of spectral mixture analysis have been developed and applied to derive accurate grainsize parameters (Painter et al., 1995; 1998). These new methods account for the nonlinear expression of grainsize in the reflected spectrum of snow. Research and analyses continue to improve and validate derivations of snow properties from AVIRIS-measured spectra.

Biomass Burning

Characteristics of the fuel, fire process, combustion products, and post-fire regrowth of biomass burning are expressed in the spectra measured by AVIRIS. From the research in ecology and vegetation, AVIRIS spectral images have been used to derive vegetation type, abundance, and leaf water. These are critical parameters for predicting susceptibility to biomass burning. In the burning process, the fire emits electromagnetic radiation as a spectral function of temperature. This spectral signature has been used to derive both the temperature and the area of burning fires with AVIRIS spectra (Green, 1996). Smoke generated from biomass burning is of local to global importance with short- and long-term impacts on the environment. Properties of smoke and associated clouds have been derived from calibrated AVIRIS spectral images (Gao et al., 1993; 1995). In the aftermath of biomass burning, the composition of the surface and regrowth may be measured and monitored. In 1995, AVIRIS measured more than 1000 spectral images with many active fires during a deployment to Brazil. Research and analysis is continuing with these and other AVIRIS biomass burning data.

Environmental Hazards

Spectral images measured by AVIRIS have been used to determine surface compositions that are directly or indirectly related to environmental hazards. For example, AVIRIS spectra were measured over the EPA superfund site at Leadville, Colorado. The spectra were used to map the distribution of acid generating minerals (Swayze et al., 1996). At Leadville, acidic water and mobilized heavy metals are an environmental hazard. The AVIRIS results at Leadville both focused and accelerated the remediation efforts at the site. AVIRIS spectra have been used to assess the transport of hazardous mine waste downstream through alluvial processes (Farrand and Harsanyi, 1995). For these applications, spectroscopy is required to accurately identify the specific mine-related minerals and separate them from naturally occurring background minerals. The mineral of interest may be the hazard or an associated tracer. Imaging is required to uniformly sample the large regions that are involved in mining and alluvial transport of mine wastes. A natural hazard associated with the volcanoes of the Cascade mountains in the western United States has been investigated. In 1996 AVIRIS spectral images were measured for most of these volcanoes. The spectra were used to map the distribution of specific alteration minerals. These alteration minerals are associated with weak zones in the volcanic slopes and are indicators of regions of slope instability and potential collapse (Crowley and Zimbelman, 1997). As communities grow near these volcanoes, understanding the hazards is of slope increasing importance. As described in biomass burning, wild fires are another environmental hazard where AVIRIS spectral images provide information for assessing risk. AVIRIS has applicability to environmental hazards where a link is established between the exposed surface composition and the human-induced or natural hazard.

Satellite Simulation and Calibration

AVIRIS spectral measurements are ideal for the simulation and calibration of multispectral satellites that are currently operating or planned. AVIRIS has been used to simulate Landsat (Kalman and Pelzer, 1993) and EOS ASTER (Abrams, 1992). In addition to simulation, AVIRIS spectral images have been used to investigate hypothesized spectral shifts in SPOT and AVHRR (Willart Soufflet and Santer, 1993; Wetzel, 1995). An AVIRIS underflight of the optical sensor (OPS) on board the Japanese Environmental Resource Satellite (JERS-1) has been used to develop an improved on orbit calibration for this spaceborne sensor (Green and Shimada, 1997). For on orbit calibration and validation objectives, AVIRIS has under flown the ADEOS satellite, and plans are in place for a series of underflights of SeaWIFS and EOS sensors. The spectral, radiometric, and geometric calibration achieved with AVIRIS to pursue research and applications is suited to validate, improve, and intercompare the calibration of satellite sensors on orbit. This is an important and growing role for AVIRIS with the planned launch of a range of satellite sensors measuring portions of the solar reflected spectrum.

Commercial Applications

Commercial applications require value be obtained from the remotely sensed data. In remote sensing, value typically comes from decisions made from information derived from data. Imaging spectroscopy derives information from the molecular absorption features and scattering characteristics expressed in a range of materials on the Earth's surface. The spectral range, calibration, and signal-to-noise of AVIRIS are well suited to derive information for commercial applications in mineral exploration (Kruse and Huntington, 1996); mine waste cleanup; agricultural crop distribution, health and yield; land use (Ray et al., 1993); forest health and regrowth, coastal and wetland environmental status, wildfire risk assessment; urban planning, etc. A new thrust at NASA for commercial applications of imaging spectroscopy is expected to acquire a number AVIRIS data sets in pursuit of these objectives.

Spectral Algorithms

Measurement of spectral images by AVIRIS has led to the development of a wide range of new algorithms to extract information from solar reflected spectra. To identify minerals with AVIRIS spectra, algorithms have been developed to measure the position, depth, and shape of mineral absorption features (Clark et al., 1990; 1991). Expert system algorithms have been developed to determine material composition from AVIRIS spectra (Kruse et al., 1992a, 1992b). Algorithms to extract information have been developed based on the projection of AVIRIS spectra in high-dimensional geometric space (Boardman, 1993). Partial spectral mixture and multiple endmember mixture algorithms have evolved to take advantage of the subtle constituent information present in the AVIRIS spectra (Boardman, 1995, Roberts et al., 1997). Multivariate analysis (Johnson et al., 1994) and cross correlaogram spectral matching (Vandermeer and Bakker, 1997) algorithms have been developed for vegetation and mineral objectives with AVIRIS spectral images. Classification algorithms have been developed to take advantage of the high spectral resolution of AVIRIS data (Hoffbeck and Landgrebe, 1996). Algorithms continue to be developed to take advantage of the information embedded in the full AVIRIS spectrum.

Compression algorithms for AVIRIS spectra have been developed to explore reduction data volume and data rates (Roger et al., 1992; Roger and Arnold, 1996; Roger and Cavenor, 1996; Ryan and Arnold, 1997). Lossless compression has the advantage that subtle spectral absorption features embedded in the AVIRIS spectra are

fully preserved. In contrast, the high compression rates of lossy compression must be evaluated in the context of the planned analysis algorithms for the specific objectives. Algorithms have also been developed to geocode AVIRIS spectral images based on the location and pointing of the sensor and the surface topography (Meyer, 1994). Geocoding is of increasing importance as derived parameters from AVIRIS are used with other data sets for research and applications.

Human Infrastructure

The range of different molecular and scattering constituents found in the urban environment and associated with human infrastructure forms a basis for use of AVIRIS spectral images. A spectroscopic approach is essential to resolve the high spatial frequency mixed spectral signatures present. For example, the spectral characteristics of impervious surfaces are separable from mixtures of natural and vegetated surfaces in the urban environment (Ridd et al., 1992). An alternate urban application example is measurement of the composition of roofs in fire hazard zones. The spectral characteristics of communication and travel routes have been measured with AVIRIS spectral images (Salu, 1995). The composition of the developed infrastructure as well as the disturbance of the natural background allowed detection and mapping of infrastructure elements. Imaging spectroscopy provides a uniform synoptic approach to mapping the surface material in the urban and adjacent environments to support characterization, monitoring, and planning.

Spectral Modeling

Models of the atmospheric and surface signatures measured by AVIRIS are essential to understanding and improving the measurements as well as deriving information from the spectra. An important model used with AVIRIS is the MODTRAN radiative transfer code (Berk et al., 1989; Anderson et al., 1995). This model has been used to validate and improve the calibration of AVIRIS through a series of inflight calibration validation experiments. Comparison of MODTRAN predicted radiance with AVIRIS measured radiance has also resulted in improvements in the MODTRAN model. For example, discrepancies were found in the exoatmospheric solar irradiance spectrum used in MODTRAN version 2 (Gao and Green, 1995). Small discrepancies currently exist in the modeling of the 1280 nm oxygen band in MODTRAN. MODTRAN is continuing to improve with recent enhancement of the cloud modeling capabilities (Berk et al., 1998). The ability of MODTRAN to accurately model the radiance spectra measured by AVIRIS allows MODTRAN to be used for inversion of parameters from AVIRIS spectra such as water vapor and surface reflectance. Other radiative transfer models have also been used to analyze and invert AVIRIS spectra (van den Bosch and Alley, 1991).

Models of the surface are used to analyze and derive parameters from AVIRIS derived reflectance spectra. Leaf and canopy models have been used to investigate and extract vegetation parameters (Conel et al., 1993a,b; Jacquemoud et al., 1995). Models parameterizing the absorption and scattering properties of water bodies have been used to predict the application of AVIRIS spectra to coastal and inland water research (Hoogenboom et al., 1998). A Planck function based model of emitted radiance as a function of temperature has been used for analysis of AVIRIS spectra measured over fires and volcanic lava. Models of the reflectance of snow as a function of grainsize have been used to derive snow properties from AVIRIS spectra. Accurate models of the absorption and scattering properties of surface materials provide an important analysis and inversion approach for extraction information from calibrated AVIRIS spectra.

CONCLUSION

Laboratory and ground based spectroscopy have been increasingly used across a range of research and applications areas. AVIRIS was developed to extend the use of spectroscopy to the realm of Earth remote sensing. AVIRIS was the first imaging spectrometer to measure the solar reflected spectrum from 400 nm to 2500 nm with contiguous 10 nm channels. The AVIRIS system was designed, developed, upgraded, and maintained to support a range of NASA research and applications objectives. The initial design of the sensor with an efficient scan mirror, f/1 spectrometers, and 200 μm detectors has enabled a series of upgrades that resulted in high signal throughput and low noise performance. A parallel set of upgrades has focused on stabilizing the spectrometers and onboard calibrator as well as developing a set of new spectral, radiometric, and spatial calibration techniques. In combination, these efforts resulted in the current accurate spectral, radiometric and spatial calibration as well as high signal-to-noise of AVIRIS. With the increased demand for AVIRIS spectral images, the data system was upgraded to take advantage of new computer and mass storage technology. This upgrade also resulted in the breakup of the monolithic AVIRIS processing program into a series of simple program modules dedicated to the calibration and distribution of each year's data. As the sensor, calibration and data system evolved, the flight operations procedures and technology were improved. These procedures ensure that AVIRIS acquires the research and application data sets requested by the investigator and that the AVIRIS sensor is performing nominally before, during, and after each flight. Both e-mail and the AVIRIS Web site now play an important role in keeping investigators informed of acquisition and performance status. The upgrades to the sensor, calibration, data system, and flight operations leave AVIRIS in a strong position to continue to support research and applications in the future.

The initial science objectives for AVIRIS were investigation of the vegetation red edge and mineral absorptions in 2200 nm spectral region. With the measurement of the solar reflected spectrum from 400 nm to 2500 nm at high spectral resolution and improved performance, investigations using AVIRIS are increasing in number, diversity, and rigor with each year of data acquisition. The high signal-to-noise and accurate calibration of AVIRIS spectral images are relevant to the full range of investigations where molecular absorptions and scattering signatures are expressed in the solar reflected spectrum.

Future spaceborne satellite sensors will measure solar reflected spectra as images in the manner established by AVIRIS. These sensors will provide access to spectral images from all regions of the Earth with multitemporal coverage. However, the altitude and velocity of satellites cause significant challenges to the measurement of high quality spectra from space. Accurate spectral, radiometric, and spatial calibration of this first generation of spaceborne imaging spectrometer will be difficult and require new approaches and capabilities. The end-to-end AVIRIS system will continue to be required to measure high quality spectral images for research and applications as well as to validate this first generation of spaceborne imaging spectrometers.

This research was carried out at the Jet Propulsion Laboratory/ California Institute of Technology, Pasadena, California, under contract with the National Aeronautics and Space Administration.

REFERENCES

Abrams, M. (1992), Simulation of ASTER using AVIRIS images. In *Summaries of the Third Annual JPL Airborne Geoscience Workshop*, JPL Publ. 92–14, Vol. 1, Jet Propulsion Laboratory, Pasadena, CA, pp. 83–84.

Anderson, G. P., Wang, J., and Chrtwynd, J. H. (1995), MODTRAN3: An update and recent validation against airborne high resolution inferometer measurements. In *Summaries of the Fifth Annual JPL Airborne Earth Science Workshop*, JPL Publ. 95–1, Vol. 1, Jet Propulsion Laboratory, Pasadena, CA, pp. 5–8.

Baugh, W. M., Kruse, F. A. (1995), Quantative remote sensing of ammonium minerals, Cedar Mountains, Esmeralda County, Nevada. In *Summaries of the Fifth Annual JPL Airborne Earth Science Workshop*, JPL Publ. 95–1, Vol. 1, Jet Propulsion Laboratory, Pasadena, CA, pp. 11–14.

Baugh, W. M., Kruse, F. A., and Atkinson, W. W. (1998), Quantitative geochemical mapping of ammonium minerals in the southern Cedar Mountains, Nevada, using the Airborne Visible/Infrared Imaging Spectrometer (AVIRIS). *Remote Sens. Environ.* 65:292–308.

Beratan, K. K., Peer, B., Dunbar, N. W., and Blom, R. (1997), A remote sensing approach to alteration mapping AVIRIS data and extension related potassium Metasomatism, Socorro, New Mexico. *Int. J. Remote Sens.* 18(17):3595–3609.

Berendes, T. A., Feind, R. E., Kuo, K. S., and Welch, R. M. (1991), Cloud base height and optical thickness retrieval, using AVIRIS data. In *Proceedings of the Third Airborne Visible/Infrared Imaging Spectrometer (AVIRIS) Workshop*, JPL Publ. 91–28, Jet Propulsion Laboratory, Pasadena, CA, pp. 232–247.

Berk, A., Bernstein, L. S., and Robertson, D. C. (1989), MODTRAN: A moderate resolution model for LOWTRAN 7, Final report, GL-TR-0122, AFGL, Hanscomb AFB, MA, 42 pp.

Berk, A., Bernstein, L. S., Anderson, G. P., et al. (1998), Modtran cloud and multiple scattering upgrades with application to AVIRIS. *Remote Sens. Environ.* 65:367–375.

Boardman, J. W. (1993), Automating spectral unmixing of AVIRIS data using geometry concepts. In *Summaries of the Fourth Annual JPL Airborne Geoscience Workshop*, JPL Publ. 93–26, Vol. 1, Jet Propulsion Laboratory, Pasadena, CA, pp. 11–14.

Boardman, J. W. (1995), Using dark current data to estimate AVIRIS noise covariance and improve spectral analyses. In *Summaries of the Fifth Annual JPL Airborne Earth Science Workshop*, JPL Publ. 93–26, Vol. 1, Jet Propulsion Laboratory, Pasadena, CA, pp. 19–22.

Boardman, J. W., and Goetz, A. F. H. (1991), Sedimentary facies analysis using AVIRIS data: a geophysical inverse problem. In *Proceedings of the Third Airborne Visible/Infrared Imaging Spectrometer (AVIRIS) Workshop*, JPL Publ. 91–28, Jet Propulsion Laboratory, Pasadena, CA, pp. 4–13.

Boardman, J. W., and Huntington, J. F. (1996), Mineral mapping with 1995 AVIRIS data. In *Summaries of the Sixth Annual JPL Airborne Earth Science Workshop*, JPL Publ. 96–4, Vol. 1, Jet Propulsion Laboratory, Pasadena, CA, pp. 9–12.

Bowers, T. L., and Rowan, L. C. (1996), Remote mineralogic and lithologic mapping of the ice river alkaline complex, British Columbia Canada, using AVIRIS data. *Photogramm. Eng. Remote Sens.* 62(12):1379–1385.

Bruegge, C. J., Conel, J. E., Green, R. O., et al. (1992), Water vapor column abundance retrievals during fire. *J. Geophys. Res. Atmos.* 97(D17):18,759–18,768.

Carder, K. L., Reinersmn, P., and Chen, R. F. (1993), AVIRIS calibration using the cloud shadow method. In *Summaries of the Fourth Annual JPL Airborne Geoscience Workshop*, JPL Publ. 93–26, Vol. 1, Jet Propulsion Laboratory, Pasadena, CA, pp. 15–18.

Carrere, V., and Abrams, M. J. (1988), An assessment of AVIRIS data for hydrothermal operation mapping in the Goldfield mining district, Nevada. In *Proceedings of the Airborne Visible/Infrared Imaging Spectrometer (AVIRIS) Performance Evaluation Workshop*, JPL Publ. 88–38, Jet Propulsion Laboratory, Pasadena, CA, pp. 134–154.

Chen, Z., Elvidge, C. D., and Groeneveld, D. P. (1992), Primary studies of trace quantities of green vegetation in Mono Lake area using 1990 AVIRIS data. In *Summaries of the Third Annual JPL Airborne Geoscience Workshop*, JPL Publ. 96–14, Vol. 1, Jet Propulsion Laboratory, Pasadena, CA, pp. 86–87.

Chen, Z., Elvidge, C. D., and Groeneveld, D. P. (1998), Monitoring seasonal dynamics of arid land vegetation using AVIRIS data. *Remote Sens. Environ.* 65:255–266.

Chrien, T. G. (1992), AVIRIS: recent instrument maintenance, modifications and 1992 performance. In *Summaries of the Third Annual JPL Airborne Geoscience Workshop*, JPL Publ. 92–14, Vol. 1, Jet Propulsion Laboratory, Pasadena, CA, pp. 78–79.

Chrien, T. G., and Green, R. O. (1993), Instantaneous field of view and spacial sampling of the Airborne Visible/Infrared Imaging Spectrometer (AVIRIS). In *Summaries of the Fourth Annual JPL Airborne Geoscience Workshop*, JPL Publ. 93–26, Vol. 1, Jet Propulsion Laboratory, Pasadena, CA, pp. 23–26.

Chrien, T. G., Green, R. O., and Eastwood, M. L. (1990), Accuracy of the spectral and radiometric laboratory calibration of the Airborne Visible/Infrared Imaging Spectrometer. In *Proceedings of the Second Airborne Visible/Infrared Imaging Spectrometer (AVIRIS) Workshop*, JPL Publ. 90–54, Jet Propulsion Laboratory, Pasadena, CA, pp. 1–14.

Chrien, T. G., Green, R. O., Sarture, C. M., Chovit, C., Eastwood, M. L., and Eng, B. T. (1993), Airborne Visible/Infrared Imaging Spectrometer (AVIRIS): recent improvements to the sensor. In *Summaries of the Fourth Annual JPL Airborne Geoscience Workshop*, JPL Publ. 93–26, Vol. 1, Jet Propulsion Laboratory, Pasadena, CA, pp. 27–30.

Chrien, T. G., Eastwood, M., Green, R. O., et al. (1995a), Airborne Visible Infrared/Visible Imaging Spectrometer (AVIRIS) onboard calibration system. In *Summaries of the Fifth Annual JPL Airborne Earth Science Workshop*, JPL Publ. 95–1, Vol. 1, Jet Propulsion Laboratory, Pasadena, CA, pp. 31–32.

Chrien, T. G., Green, R. O., Chovit, C., and Hajek, P. (1995b), New calibration techniques for the Airborne Visible/Infrared Imaging Spectrometer (AVIRIS). In *Summaries of the Fifth Annual JPL Airborne Earth Science Workshop*, JPL Publ. 95–1, Vol. 1, Jet Propulsion Laborary, Pasadena, CA, pp. 33–34.

Clark, R. N., Gallagher, A. J., and Swayze, G. (1990), Material absorption band depth mapping of imaging spectrometer data using a complete band shape least squares fit with library reference spectra. In *Proceedings of the Second Airborne Visible/Infrared Imaging Spectrometer (AVIRIS) Workshop*, JPL Publ. 90–54, Jet Propulsion Laboratory, Pasadena, CA, pp. 176–186.

Clark, R. N., Swayze, G. A., Gallagher, A., Gorelick, N., and Kruse, F. (1991), Mapping with imaging spectrometer data using complete band shape least squares algorithm simultaneously fit to multiple spectral features from multiple materials. In *Proceedings of the Third Airborne Visible/Infrared Imaging Spectrometer (AVIRIS) Workshop*, JPL Publ. 91–28, Jet Propulsion Laboratory, Pasadena, CA, pp. 2–3.

Clark, R. N., Swayze, G., and Gallagher, A. (1992), Mapping the minerology and lithiology of Canyonlands, Utah with imaging spectrometer data and multiple spectral feature mapping algorithm. In *Summaries of the Third Annual JPL Airborne Geoscience Workshop*, JPL Publ. 92–14, Vol. 1, Jet Propulsion Laboratory, Pasadena, CA, pp. 11–13.

Clark, R. N., Swayze, G. A., Heidebrecht, K., Green, R. O., and Goetz, A. F. H. (1995), Calibration to surface reflectance of terrestrial imaging spectrometry data: comparing methods. In *Summaries of the Fifth Annual JPL Airborne Earth Science Workshop*, JPL Publ. 95–1, Vol. 1, Jet Propulsion Laboratory, Pasadena, CA, pp. 41–42.

Clevers, J. G. P. W., Buker, C., Vanleeuwen, H. J. C., and Bouman, B. A. M. (1994), A framework for monitoring crop growth by combining directional and spectral remote sensing information. *Remote Sens. Environ.* 50(2):161–170.

Conel, J. E., Green, R. O., Alley, R. E., et al. (1988a), In flight radiometric calibration of the Airborne Visible/Infrared Imaging Spectrometer (AVIRIS). In *Proceedings of the SPIE Conference on Recent Advances in Sensors, Radiometry and Data Processing for Remote Sensing*, Orlando, FL, 4–8 April, p. 924.

Conel, J. E., Green, R. O., Carrere, et al. (1988b), Atmospheric water mapping with the Airborne Visible/Infrared Imaging Spectrometer (AVIRIS). In *Proceedings of the Airborne Visible/Infrared Imaging Spectrometer (AVIRIS) Performance Evaluation Workshop*, JPL Publ. 88–38, Jet Propulsion Laboratory, Pasadena, CA, pp. 21–29.

Conel, J. E., van den Bocsh, J., and Grove, C. I. (1993a), Application of a two stream radiative transfer model for leaf lignin and cellulose concentrations from spectral reflectance measurements (Part 1). In *Summaries of the Fourth Annual JPL Airborne Geoscience Workshop*, JPL Publ. 93–28, Vol. 1, Jet Propulsion Laboratory, Pasadena, CA, pp. 39–44.

Conel, J. E., van den Bocsh, J., and Grove, C. I. (1993b), Application of a two stream radiative transfer model for leaf lignin and celluose concentrations from spectral reflectance measurements (Part 2). In *Summaries of the Fourth Annual JPL Airborne Geoscience Workshop*, JPL Publ. 93–26, Vol. 1, Jet Propulsion Laboratory, Pasadena, CA, pp. 45–52.

Crosta, A. P., Sabine, C., and Taranik, J. V. (1998), A comparison of image processing methods for alteration mapping at Bodie, California, Using 1992 AVIRIS Data. *Remote Sens. Environ.* 65;309–319.

Crowley, J. K. (1993), Mapping playa evaporite minerals with AVIRIS data. *Remote Sens. Environ.* 44(2–3):337–356.

Crowley, J. K., and Zimbelman, D. R. (1997), Mapping hydrothermally altered rocks on Mount Rainier, Washington, with Airborne Visible/Infrared Imaging Spectrometer (AVIRIS) Data. *Geology* 25(6):559–562.

Curran, P. J., Kupiec, J. A., and Smith, G. M. (1997), Remote sensing the biochemical composition of a slash pine canopy. *IEEE Trans. Geosci. Remote Sens.* 35(2):415–420.

Elvidge, C.D. (1988), Examination of the spectral features of vegetation in 1987 AVIRIS data. In *Proceedings of the Airborne Visible/Infrared Imaging Spectrometer (AVIRIS) Performance Evaluation Workshop*, JPL Publ. 88–38, Jet Propulsion Laboratory, Pasadena, CA, pp. 97–101.

Elvidge, C. D. (1990), Detection of trace quantities of green vegetation in the 1989 AVIRIS data. In *Proceedings of the Second Airborne Visible/Infrared Imaging Spectrometer (AVIRIS) Workshop*, JPL Publ. 90–54, Jet Propulsion Laboratory, Pasadena, CA, pp. 35–41.

Elvidge, C. D., Chen, Z. K., and Groeneveld, D. P. (1993), Detection of trace quantities of green vegetation 1990 AVIRIS data. *Remote Sens. Environ.* 44(2–3):271–279.

Farrand, W. H. (1997), Identification and mapping of ferric oxide and oxyhydroxide minerals in imaging spectrometer data of Summitville, Colorado, USA, and the surrounding San Juan Mountains. *Int. J. Remote Sens.* 18(7):1543–1552.

Farrand, W. H., and Harsanyi, J. C. (1995), Minerologic variations in fluvial sediments contaminated by mine tailings as determined by AVIRIS data, Coeur d'Alene River Valley, Idaho. In *Summaries of the Fifth Annual JPL Airborne Earth Science Workshop*, JPL Publ. 95–1, Vol. 1, Jet Propulsion Laboratory, Pasadena, CA, pp. 47–50.

Farrand, W. H., Singer, R. B., and Mereínyi, E. (1994), Retrieval of apparent surface reflectance from AVIRIS data a comparison of emperical line, radiative transfer, and spectral mixture methods. *Remote Sens. Environ.* 47(3):311–321.

Feind, R. E., and Welch, R. M. (1995), Cloud fraction and cloud shadow property retrievals from coregistered TIMS and AVIRIS imagery: the use of cloud morphology for registration. *IEEE Trans. Geosci. Remote Sens.* 33(1):172–184.

Ferrier, G., and Wadge, G. (1996), The application of imaging spectrometry data to mapping alteration zones associated with gold mineralization in Southern Spain. *Int. J. Remote Sens.* 17(2):331–350.

Fischer, A. F. (1991), Mapping and correlating desert soils and surfaces with imaging spectrometry. In *Proceedings of the Third Airborne Visible/Infrared Imaging Spectrometer (AVIRIS) Workshop*, JPL Publ. 91–28, Jet Propulsion Laboratory, Pasadena, CA, pp. 23–32.

Fox, L., Fischer, A. F., Gillespie, A. R., and Smith, M. R. (1990), Using spectral mixture analysis of AVIRIS high dimensional data for distinguishing soil consequences. In *Proceedings of the Second Airborne Visible/Infrared Imaging Spectrometer (AVIRIS) Workshop*, JPL Publ. 90–54, Jet Propulsion Laboratory, Pasadena, CA, pp. 94–99.

Gaddis, L. R., Soderblom, L. A., Kieffer, H. H., et al. (1996), Decomposition of AVIRIS spectra extraction of surface reflectance, atmospheric, and instrumental components. *IEEE Trans. Geosci. Remote Sens.* 34(1):163–178.

Gamon, J. A., Field, C. B., and Ustin, S. L. (1992), Evaluation of spatial productivity patterns in an annual grassland during an AVIRIS overflight. In *Summaries of the Third Annual JPL Airborne Geoscience Workshop*, JPL Publ. 92–14, Vol. 1, Jet Propulsion Laboratory, Pasadena, CA, pp. 17–19.

Gao, B. C., and Goetz, A. F. H. (1990), Determination of a cloud area from AVIRIS data. In *Proceedings of the Second Airborne Visible/Infrared Imaging Spectrometer (AVIRIS) Workshop*, JPL Publ. 90–54, Jet Propulsion Laboratory, Pasadena, CA, pp. 157–161.

Gao, B. C., and Goetz, A. F. H. (1992), Separation of cirrus clouds from clear surface from AVIRIS data using the 1.38 μm water vapor band. In *Summaries of the Third Annual JPL Airborne Geoscience Workshop*, JPL Publ. 92–14, Vol. 1, Jet Propulsion Laboratory, Pasadena, CA, pp. 98–100.

Gao, B. C., and Goetz, A. F. H. (1994), Extraction of dry leaf spectral features from reflectance spectra of green. *Remote Sens. Environ.* 47(3):369–374.

Gao, B. C., and Goetz, A. F. H. (1995), Retrieval of equivalent water thickness and information related to biochemical components of vegetation canopies from AVIRIS data. *Remote Sens. Environ.* 52(3):155–162.

Gao, B. C., and Kaufman, Y. J. (1995), Correction of thin cirrus effects in AVIRIS images using the sensitive 1.375 μm cirrus detecting channel. In *Summaries of the Fifth Annual JPL Airborne Earth Science Workshop*, JPL Publ. 95–1, Vol. 1, Jet Propulsion Laboratory, Pasadena, CA, pp. 59–62.

Gao, B. C., Goetz, A. F. H., and Zamudio, J. A. (1991a), Removing atmospheric effects from AVIRIS data for surface reflectance retrievals. In *Proceedings of the Third Airborne Visible/Infrared Imaging Spectrometer (AVIRIS) Workshop*, JPL Publ. 91–28, Jet Propulsion Laboratory, Pasadena, CA, pp. 80–86.

Gao, B. C., Kierein-Young, K. S., Goetz, A. F. H., et al. (1991b), Case studies of water vapor and surface liquid water from AVIRIS data measured over Denver, CO, and Death Valley, CA. In *Proceedings of the Third Airborne Visible/Infrared Imaging Spectrometer (AVIRIS) Workshop*, JPL Publ. 91–28, Jet Propulsion Laboratory, Pasadena, CA, pp. 222–231.

Gao, B. C., Kaufman, Y. J., and Green, R. O. (1993), Remote sensing of smoke, clouds, and fire using AVIRIS data. In *Summaries of the Fourth Annual JPL Airborne Geoscience Workshop*, JPL Publ. 93–26, Vol. 1, Jet Propulsion Laboratory, Pasadena, CA, pp. 61–64.

Gao, B. C., Remer, L., and Kaufman, Y. J. (1995), Remote sensing of smoke, clouds, and radiation using AVIRIS during SCAR experiments. In *Summaries of the Fifth Annual JPL Airborne Earth Science Workshop*, JPL Publ. 95–1, Vol. 1, Jet Propulsion Laboratory, Pasadena, CA, pp. 63–66.

Gao, B. C., and Green R. O. (1995), Presence of terrestrial atmospheric gas-absorption bands in standard extraterrestrial solar irradiance curves in the near-infrared spectral region. *App. Optics* 34:6263–6268.

Garciaharo, F. J., Gilabert, M. A., and Melia, J. (1996), Linear spectral mixture modeling to estimate vegetation amount from optical spectral data. *Int. J. Remote Sens.* 17(17):3373–3400.

Gastellu-Etchegorry, J. P., Zagolski, F., Marty, G., and Giordano, G. (1995), An assessment of canopy chemistry with AVIRIS: A case study in the Landes Forest, South West France. *Int. J. Remote Sens.* 16(3):487–501.

Green, R. O., Ed. (1990a), *Proceedings of the Second Airborne Visible/Infrared Imaging Spectrometer (AVIRIS) Workshop*, JPL Publ. 90–54, Jet Propulsion Laboratory, Pasadena, CA, 280 pp.

Green, R. O. (1990b), Retrieval of reflectance from calibrated radiance imagery measured by the airborne visible/infrared imaging spectrometer (AVIRIS) for lithological mapping of the Clark Mountains, California. In *Proceedings of the Second Airborne Visible/Infrared Imaging Spectrometer (AVIRIS) Workshop*, JPL Publ. 90–54, Jet Propulsion Laboratory, Pasadena, CA, pp. 167–175.

Green, R. O., Ed. (1991), *Proceedings of the Third Airborne Visible/Infrared Imaging Spectrometer (AVIRIS) Workshop*, JPL Publ. 91–28, Jet Propulsion Laboratory, Pasadena, CA, 326 pp.

Green, R. O., Ed. (1992), *Summaries of the Third Annual JPL Airborne Geoscience Workshop, Vol 1. AVIRIS*, JPL Publ. 92–14, Jet Propulsion Laboratory, Pasadena, CA, 159 pp.

Green, R. O., Ed. (1993), *Summaries of the Fourth Annual JPL Airborne Geoscience Workshop, Vol 1. AVIRIS*, JPL Publ. 93–26, Jet Propulsion Laboratory, Pasadena, CA, 209 pp.

Green, R. O., Ed. (1995), *Summaries of the Fifth Annual JPL Airborne Earth Science Workshop, Vol 1. AVIRIS*, JPL Publ. 95–1, Jet Propulsion Laboratory, Pasadena, CA, 161 pp.

Green, R. O., Ed. (1996a), *Summaries of the Fifth Annual JPL Airborne Earth Science Workshop, Vol 1. AVIRIS*, JPL Publ. 96–4, Jet Propulsion Laboratory, Pasadena, CA, 238 pp.

Green, R. O. (1996b), Estimation of biomass fire temperature and areal extent from calibrated AVIRIS spectra. In *Summaries of the Sixth Annual JPL Airborne Earth Science Workshop*, JPL Publ. 96–4, Vol. 1, Jet Propulsion Laboratory, Pasadena, CA, pp. 105–114.

Green, R. O., and Conel, J. E. (1995) Movement of water vapor in the atmosphere measured by an imaging spectrometer at Rogers Dry Lake, CA. In *Summaries of the Fifth Annual JPL Airborne Earth Science Workshop*, JPL Publ. 96–4, Vol. 1, Jet Propulsion Laboratory, Pasadena, CA, pp. 87–90.

Green, R. O., and Dozier, J. (1995), Measurement of the spec-

tral absorption of liquid water in melting snow with and imaging spectrometer. In *Summaries of the Fifth Annual JPL Airborne Earth Science Workshop*, JPL Publ. 96–4, Vol. 1, Jet Propulsion Laboratory, Pasadena, CA, pp. 91–94.

Green, R. O., and Dozier, J. (1996), Retrieval of surface snow grain size and melt water from AVIRIS spectra. In *Summaries of the Sixth Annual JPL Airborne Earth Science Workshop*, JPL Publ. 96–4, Vol. 1, Jet Propulsion Laboratory, Pasadena, CA, pp. 127–134.

Green, R. O., and Shimada, M. (1997), On-orbit calibration of a multispectral satellite sensor using a high-altitude airborne imaging spectrometer. *Adv. Space Res.* 19(9):1387–1398.

Green, R. O., Vane, G. A., and Conel, J. L. (1988), Determination of in flight AVIRIS spectral, radiometric, spatial, and signal to noise characteristics using atmospheric and surface measurements from the vicinity of the rare earth bearing carbonatite at Mountain Pass, California. In *Proceedings of the Airborne Visible/Infrared Imaging Spectrometer (AVIRIS) Performance Evaluation Workshop*, JPL Publ. 88–38, Jet Propulsion Laboratory, Pasadena, CA, pp. 162–184.

Green, R. O., Conel J. E., Carrere, V., et al. (1990), Inflight validation and calibration of the spectral and radiometric characteristics of the airborne visible/infrared imaging spectrometer (AVIRIS). In *Proceedings of the SPIE Conference on Aerospace Sensing, Imaging Spectroscopy of the Terrestrial Environment*, Orlando, FL, 16–20 April, pp. 18–36.

Green, R. O., Conel, J. E., Margolis, J. S., Bruege, C. J., and Hoover, G. L. (1991), An inversion algorithm for retrieval of atmospheric and leaf water absorption from AVIRIS radience with compensation for atmospheric scattering. In *Proceedings of the Third Airborne Visible/Infrared Imaging Spectrometer (AVIRIS) Workshop*, JPL Publ. 91–28, Jet Propulsion Laboratory, Pasadena, CA, pp. 51–61.

Green, R. O., Conel, J. E., and Roberts, D. A. (1993), Estimation of aerosol optical depth and additional atmospheric parameters for the calculation of the reflectance from radience measured by the Airborne Visible/Infrared Imaging Spectrometer. In *Summaries of the Fourth Annual JPL Airborne Geoscience Workshop*, JPL Publ. 93–26, Vol. 1, Jet Propulsion Laboratory, Pasadena, CA, pp. 73–76.

Green, R. O., Conel, J. E., Helmlinger, M., van den Bosch, J., and Hajek, P. (1996), In-flight radiometric calibration of AVIRIS in 1994. In *Summaries of the Sixth Annual JPL Airborne Earth Science Workshop*, JPL Publ. 96–4, Vol. 1, Jet Propulsion Laboratory, Pasadena, CA.

Hoffbeck, J. P., and Landgrebe, D. A. (1996), Classification of remote sensing images having high spectral resolution. *Remote Sens. Environ.* 57(3):119–126.

Hoogenboom, H. J., Dekker, A. G., and Althuis, I. J. A. (1998), Simulation of AVIRIS performance for detecting chlorophyll over coastal and inland waters. *Remote Sens. Environ.* 65:333–340.

Hook, S. J., and Rast, M. (1990), Mineralogic mapping using Airborne Visible/Infrared Imaging Spectrometer (AVIRIS) shortwave infrared (SWIR) data acquired over Cuprite, Nevada. In *Proceedings of the Second Airborne Visible/Infrared Imaging Spectrometer (AVIRIS) Workshop*, JPL Publ. 90–54, Jet Propulsion Laboratory, Pasadena, CA, pp. 199–207.

Hutchison, K. D., and Choe, N. J. (1996), Application of 1 center dot 38 μm imagery for thin cirrus detection in daytime imagery collected over land surfaces. *Int. J. Remote Sens.* 17(17):3325–3342.

Isakov, V. Y., Feind, R. E., Vasilyev, O. B., and Welch, R. M. (1996), Retrieval of aerosol spectral optical thickness from AVIRIS data. *Int. J. Remote Sens.* 17(11):2165–2184.

Jacquemoud, S., Ustin, S. L., Verdebout, J., Schmuck, G., Andreoli, G., and Hosgood, B. (1995), Prospect redux. In *Summaries of the Fifth Annual JPL Airborne Earth Science Workshop*, JPL Publ. 95–1, Vol. 1, Jet Propulsion Laboratory, Pasadena, CA, pp. 99–104.

Jaquet, J. M., Schanz, F., Bossard, P., Hanselmann, K., and Gendre, F. (1994), Measurements and significance of biooptical parameters for remote sensing in 2 sub alpine lakes of different trophic state. *Aquat. Sci.* 56(3):263–305.

Johnson, L. F., Hlavka, C. A., and Peterson, D. L. (1994), Multivariate analysis of AVIRIS data for canopy biochemical estimation along the Oregon transect. *Remote Sens. Environ.* 47(2):216–230.

Kalman, L. S., and Pelzer, G. R. (1993), Simulation of landsat thematic mapper imagery using AVIRIS hyperspectral imagery. In *Summaries of the Fourth Annual JPL Airborne Geoscience Workshop*, JPL Publ. 93–26, Vol. 1, Jet Propulsion Laboratory, Pasadena, CA, pp. 97–100.

Kaufman, Y. J., Wald, A. E., Remer, L. A., et al. (1997), The modis 2.1 μm channel correlation with visible reflectance for use in remote sensing of aerosol. *IEEE Trans. Geosci. Remote Sens.* 35(5):1286–1298.

Kiereinyoung, K. S. (1997), The integration of optical and radar data to characterize mineralogy and morphology of surfaces in Death Valley, California, USA. *Int. J. Remote Sens.* 18(7):1517–1541.

Kruse, F. A., and Huntington, J. F. (1996), The 1995 AVIRIS geology group shoot. In *Summaries of the Sixth Annual JPL Airborne Earth Science Workshop*, JPL Publ. 96–4, Vol. 1, Jet Propulsion Laboratory, Pasadena, CA, pp. 155–164.

Kruse, F. A., Lefkoff, A. B., Boardman, J. W., et al. (1992a), The spectral image processing system (SIPS) software for integrated analysis of AVIRIS data. In *Summaries of the Third Annual JPL Airborne Geoscience Workshop*, JPL Publ. 92–14, Vol. 1, Jet Propulsion Laboratory, Pasadena, CA, pp. 23–25.

Kruse, F. A., Lefkoff, A. B., and Dietz, J. B. (1992b), Expert system-based mineral mapping using AVIRIS. In *Summaries of the Third Annual JPL Airborne Geoscience Workshop*, JPL Publ. 92–14, Vol. 1, Jet Propulsion Laboratory, Pasadena, California, pp. 19–21.

Kuo, K. S., Welch, R. M., Gao, B. C., and Goetz, A. F. H. (1990), Cloud identification and optical thickness retrieval using AVIRIS data. In *Proceedings of the Second Airborne Visible/Infrared Imaging Spectrometer (AVIRIS) Workshop*, JPL Publ. 90–54, Jet Propulsion Laboratory, Pasadena, CA, pp. 149–156.

Kupiec, J. A., and Curran, P. J. (1995), Decoupling the effects of the canopy and foliar biochemicals in AVIRIS spectra. *Int. J. Remote Sens.* 16(9):1731–1739.

Lacapra, V. C., Melack, J. M., Gastil, M., and Valeriano, D. (1996), Remote sensing of foliar chemistry of inundated rice with imaging spectrometry. *Remote Sens. Environ.* 55(1):50–58.

Lang, H. R., and Cabral Cano, E. (1996), Preliminary analysis of AVIRIS data for tectonostratigraphic assesment of Northern Guerrero State, Southern Mexico. In *Summaries of the*

Sixth Annual JPL Airborne Earth Science Workshop, Jet Propulsion Laboratory, Pasadena, CA, pp. 165–166.

Leprieur, C., Carrere, V., and Gu, X. F. (1995), Atmospheric corrections and ground relectance recovery for airborne visible/infrared imaging spectrometer (AVIRIS) data, MAC Europe 91. *Photogramme. Eng. Remote Sens.* 61(10):1233–1238.

Macenka, S. A., and Chrisp, M. P. (1987), *Airborne Visible/Infrared Imaging Spectrometer (AVIRIS) Spectrometer Design and Performance*, JPL Publ. 87-38, Jet Propulsion Laboratory, Pasadena, CA.

Martin, M. E., and Aber, J. D. (1993), Measurements of canopy chemistry with 1992 Aviris data at Blackhawk Island and Harvard Forest. In *Summaries of the Fourth Annual JPL Airborne Geoscience Workshop*, Jet Propulsion Laboratory, Pasadena, CA, pp. 113–116.

Martin, M. E., and Aber, J. D. (1997), High spectral resolution remote sensing of forest canopy lignin, nitrogen, and ecosystem processes. *Ecol. Appl.* 7(2):431–443.

Martin, M. E., Newman, S. D., Aber, J. D., and Congalton, R. G. (1998), Determining forest species composition using high spectral resolution remote sensing data. *Remote Sens. Environ.* 65:249–254.

Melack, J. M., and Gastil, M. (1992), Seasonal and satial variations in phytoplanktonic chlorophyll in Eutrophic Mono Lake, California, measured with the airborne visible and infrared imaging spectrometer (AVIRIS). In *Summaries of the Third Annual JPL Airborne Geoscience Workshop*, Jet Propulsion Laboratory, Pasadena, CA, pp. 53–55.

Meyer, P. (1994), A parametric approach for the geocoding of airborne visible infrared imaging spectrometer (AVIRIS) data in rugged terrain. *Remote Sens. Environ.* 49(2):118–130.

Miller, D. C. (1987), *AVIRIS Scan Drive Design and Performance*, JPL Publ. 87-38, Jet Propulsion Laboratory, Pasadena, CA.

Mustard, J. F. (1993), Relationships of soil, grass, and bedrock over the Kaweah Serpentinite Melange through spectral mixture analysis of AVIRIS data. *Remote Sens. Environ.* 44(2–3):293–308.

Nolin, A. W., and Dozier, J. (1993), Estimating snow grain size using AVIRIS data. *Remote Sens. Environ.* 44(2–3):231–238.

Novo, E., Gastil, M., and Melack, J. (1995), An algorithm for chlorophyll using first difference transformations of AVIRIS reflectance spectra. In *Summaries of the Fifth Annual JPL Airborne Earth Science Workshop*, Jet Propulsion Laboratory, Pasadena, CA, pp. 121–124.

Oppenheimer, C., Rothery, D. A., Pieri, D. C., Abrams, M. J., and Carrere, V. (1993), Analysis of airborne visible/infrared imaging spectrometer (AVIRIS) data of volcanic hot spots. *Int. J. Remote Sens.* 14(16):2919–2934.

Painter, T. H., Roberts, D. A., Green, R. O., and Dozier, J. (1995), Improving alpine region spectral unmixing with optimal fit snow endmembers. In *Summaries of the Fifth Annual JPL Airborne Earth Science Workshop*, Jet Propulsion Laboratory, Pasadena, CA, pp. 125–128.

Painter, T. H., Roberts, D. A., Green, R. O., and Dozier, J. (1998), Improving mixture analysis estimates of snow-covered-area from AVIRIS data. *Remote Sens. Environ.* 65: 320–332.

Palacios-Orueta, A., Ustin, S. L. (1996), Multivariate statistical classification of soil spectra. *Remote Sens. Environ.* 57(2): 108–118.

Pilorz, S. H., and Davis, C. O. (1990), Investigation of ocean reflectance with AVIRIS data. In *Proceedings of the Second Airborne Visible/Infrared Imaging Spectrometer (AVIRIS) Workshop*, Jet Propulsion Laboratory, Pasadena, CA, pp. 224–231.

Price, J. C. (1993), Spectral variations in a collection of AVIRIS imagery. In *Summaries of the Fourth Annual JPL Airborne Geoscience Workshop*, Jet Propulsion Laboratory, Pasadena, CA, pp. 141–144.

Price, J. C. (1995), Examples of high resolution visible to near infrared reflectance spectra and a standardized collection for remote sensing studies. *Int. J. Remote Sens.* 16(6):993–1000.

Ray, T. W., Farr, T. G., Blom, R. G., and Crippen, R. E. (1993), Monitoring land use and degradation using satellite and airborne data. In *Summaries of the Fourth Annual JPL Airborne Geoscience Workshop*, Jet Propulsion Laboratory, Pasadena, CA, pp. 145–148.

Richardson, L. L., Buisson, D., Liu, C. J., and Ambrosia, V. (1994), The detection of algal photosynthetic accessory pigments using airborne visible/infrared imaging spectrometer (AVIRIS) spectral data. *Marine Technol. Soc. J.* 28(3):10–21.

Ridd, M. K., Ritter, N. D., Bryant, N. A., and Green, R. O. (1992), AVIRIS data and neural networks applied to an urban ecosystem. In *Summaries of the Third Annual JPL Airborne Geoscience Workshop.*, JPL Publ. 92–14, Vol. 1, Jet Propulsion Laboratory, Pasadena, California, pp. 29–31.

Roberts, D. A., Smith, M. O., Adams, J. B., Sabol, D. E., Gillespie, A. R., and Willis, S. C. (1990), Isolating woody plant material and senescent vegetation from green vegetation in AVIRIS data. In *Proceedings of the Second Airborne Visible/Infrared Imaging Spectrometer (AVIRIS) Workshop*, Jet Propulsion Laboratory, Pasadena, CA, pp. 42–57.

Roberts, D. A., Green, R. O., Sabol, D. E., and Adams, J. B. (1993), Temporal changes in endmember abundances, liquid water and water vapor over vegetation at Jasper Ridge. In *Summaries of the Fourth Annual JPL Airborne Geoscience Workshop*, Jet Propulsion Laboratory, Pasadena, CA, pp. 153–156.

Roberts, D. A., Green, R. O., and Adams, J. B. (1997), Temporal and spatial patterns in vegetation and atmospheric properties from AVIRIS. *Remote Sens. Environ.* 62(3):223–240.

Roberts, D. A., Gardner, M., Church, R., Ustin S., Scheer, G., and Green, R. O. (1998), Mapping chaparral in the Santa Monica Mountains using multiple end member spectral mixture models. *Remote Sens. Environ.* 65:267–279.

Roger, R. E., and Arnold, J. F. (1996), Reliability estimating the noise in AVIRIS images. *Int. J. Remote Sens.* 17(10): 1951–1962.

Roger, R. E., and Cavenor, M. C. (1996), Lossless compression of AVIRIS images. *IEEE Trans. Image Process.* 5(5):713–719.

Roger, R. E., Arnold, J. F., Cavenor, M. C., and Richards, J. A. (1992), Lossless compression of AVIRIS data: comparison of methods and instrument constraints. In *Summaries of the Third Annual JPL Airborne Geoscience Workshop*, Jet Propulsion Laboratory, Pasadena, CA, pp. 154–156.

Rowan, L. C., Bowers, T. L., Crowley, J. K., et al. (1995), Analysis of airborne visible/infrared imaging spectrometer (AVIRIS) data of the Iron Hill, Colorado, carbonatite alkalic igneous complex. *Econ. Geol. Bull. Soc. Econ. Geol.* 90(7):1966–1982.

Ryan, M. J., and Arnold, J. F. (1997), The lossless compression

of AVIRIS images by vector quantinization. *IEEE Trans. Geosci. Remote Sens.* 35(3):546–550.

Sabol, D. E., Roberts, D. A., Adams, J. B., and Smith, M. O. (1993), Mapping and monitering changes in vegetation communities of Jasper Ridge, CA, using spectral fractions derived from AVIRIS images. In *Summaries of the Fourth Annual JPL Airborne Geoscience Workshop*, Jet Propulsion Laboratory, Pasadena, CA, pp. 157–160.

Salu, Y. (1995), Sub pixel localization of highways in AVIRIS images. In *Summaries of the Fifth Annual JPL Airborne Earth Science Workshop*, Jet Propulsion Laboratory, Pasadena, CA, pp. 137–140.

Sandidge, J. C., and Holyer, R. J. (1998), Coastal Bathymetry from Hyperspectral observations of water radiance. *Remote Sens. Environ.* 65:341–352.

Sarture, C. M., Chrien, T. G., Green, R. O., et al. (1995), Airborne visible/infrared imaging spectrometer (AVIRIS): sensor improvements for 1994 and 1995. In *Summaries of the Fifth Annual JPL Airborne Earth Science Workshop*, Jet Propulsion Laboratory, Pasadena, CA, pp. 145–148.

Schläpfer, D., Borel, C. C., Keller, J., and Itten, K. I. (1998), Atmospheric precorrected differential absorption technique to retrieve columnar water vapor. *Remote Sens. Environ.* 65:353–366.

Smith, G. M., and Curran, P. J. (1996), The signal to noise ratio (SNR) required for the estimation of foliar biochemical concentrations. *Int. J. Remote Sens.* 17(5):1031–1058.

Sommer, S., Lorcher, G., and Endres, S. (1993), Application of MAC Europe AVIRIS data to the analysis of various alteration stages in the landdmannalaugar hydrothermal area (South Iceland). In *Summaries of the Fourth Annual JPL Airborne Geoscience Workshop*, Jet Propulsion Laboratory, Pasadena, CA, pp. 165–168.

Staenz, K., Williams, D. J., Truchon, M., and Fritz, R. (1993), Estimation of crown closure from AVIRIS data using regression analysis. In *Summaries of the Fourth Annual JPL Airborne Geoscience Workshop*, Jet Propulsion Laboratory, Pasadena, CA, pp. 169–172.

Staenz, K., Williams, D. J., and Walker, B. (1996), Surface reflectance retrieval from AVIRIS data using a six dimensional look up table. In *Summaries of the Sixth Annual JPL Airborne Earth Science Workshop*, Jet Propulsion Laboratory, Pasadena, CA, pp. 223–230.

Swayze, G., Clark, R. N., Kruse, F., Sutley, S., and Gallagher, A. (1992), Ground truthing AVIRIS mineral mapping at Cuprite, Nevada. In *Summaries of the Third Annual JPL Airborne Geoscience Workshop*, Jet Propulsion Laboratory, Pasadena, CA, pp. 47–49.

Swayze, G. A., Clark, R. N., Pearson, R. M., and Livo, K. E. (1996), Mapping acid generating minerals at the California gulch superfund site in Leadville, Colorado using imaging spectroscopy. In *Summaries of the Sixth Annual JPL Airborne Earth Science Workshop*, Jet Propulsion Laboratory, Pasadena, CA, pp. 231–234.

Teillet, P. M., Staenz, K., and Williams, D. J. (1997), Effects of spectral, spatial, and radiometric characteristics on remote sensing vegetation indexes of forested regions. *Remote Sens. Environ.* 61(1):139–149.

Ustin, S. L., Smith, M. O., Roberts, D., Gamon, J. A., and Field, C. B. (1992), Using AVIRIS images to measure temporal trends, in abundance of nonphotosynthetic canopy components. In *Summaries of the Third Annual JPL Airborne Geoscience Workshop*, Jet Propulsion Laboratory, Pasadena, CA, pp. 5–7.

Ustin, S. L., Hart, Q. J., Duan, L., and Scheer, G. (1996), Vegetation mapping on hardwood rangelands in California. I. J. Remote Sens. 17:3015–3036.

Ustin, S. L., Roberts, D. A., Pinzon, J., Jacquemoud, S., Gardner, M., Scheer, G., Castaneda, C. M., and Palacios-Orueta, A. (1998), Estimating canopy water content of chaparral shrubs using optical methods. *Remote Sens. Environ.* 65:280–291.

van den Bosch, J. M., and Alley, R. E. (1991), Quantitative analysis of three atmospheric correction models for airborne visible/infrared imaging spectrometer (AVIRIS) data. In *Proceedings of the Third Airborne Visible/Infrared Imaging Spectrometer (AVIRIS) Workshop*, Jet Propulsion Laboratory, Pasadena, CA, pp. 87–95.

van den Bosch, J., Davis, C. O., Mobley, C. D., and Reah, W. J. (1993), Atmospheric correction of AVIRIS data of Monterey Bay contaminated by thin cirrus clouds. In *Summaries of the Fourth Annual JPL Airborne Geoscience Workshop*, Jet Propulsion Laboratory, Pasadena, CA, pp. 185–188.

Vandermeer, F., and Bakker, W. (1997), Cross correlogram spectral matching application to surface minerological mapping by using AVIRIS data from Cuprite, Nevada. *Remote Sens. Environ.* 61(3):371–382.

Vane, G., Ed. (1988), *Proceedings of the Airborne Visible/Infrared Imaging Spectrometer (AVIRIS) Performance Evaluation Workshop*, JPL Publ. 88-38, Jet Propulsion Laboratory, 235 pp.

Vane, G., Ed. (1993), *Airborne Imaging Spectrometry, Special Issue, Remote Sens. Environ.* 44(2–3):117–356.

Wessman, C. A., Bateson, C. A., Curtiss, B., and Benning, T. L. (1993), A comparison of the spectral mixture analysis and NDVI for ascertaining ecological variables. In *Summaries of the Fourth Annual JPL Airborne Geoscience Workshop*, Jet Propulsion Laboratory, Pasadena, CA, pp. 193–195.

Wessman, C. A., Bateson, C. A., and Benning T. L. (1997), Detecting fire and grazing patterns in tallgrass prairie using spectral mixture analysis. *Ecol. Appl.* 7(2):493–511.

Wetzel, M. A. (1995), Simulation of radiances for future AVHRR platforms with the AVIRIS spectral radiometer. *Int. J. Remote Sens.* 16(6):1167–1177.

Willart Soufflet, V., and Santer, R. (1993), Using AVIRIS for in flight calibration of the spectral shifts of spot HRV and of AVHRR. In *Summaries of the Fourth Annual JPL Airborne Geoscience Workshop*, Jet Propulsion Laboratory, Pasadena, CA, pp. 197–200.

Zagolski, F., and Gastellu-Etchegorry, J. P. (1995), Atmospheric corrections of AVIRIS images with a procedure based on the inversion of the 5S model. *Int. J. Remote Sens.* 16(16): 3115–3146.